C.P. No. 216
(17,791)
A.R.C. Technical Report

C.P. No. 216
(17,791)
A.R.C. Technical Report

MINISTRY OF SUPPLY

AERONAUTICAL RESEARCH COUNCIL

CURRENT PAPERS

Wind Tunnel Tests on a 6 ft Diameter Helicopter Rotor

By

T. B. Owen, R. Fail and R. C. W. Eyre

LONDON: HER MAJESTY'S STATIONERY OFFICE

1955

Price 3s. 6d. net

R 13,662

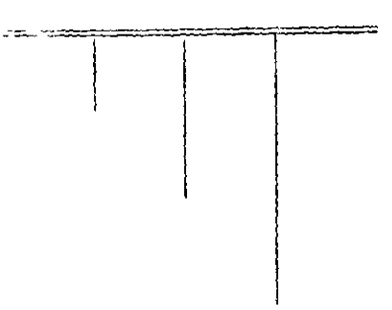

C.P. No. 216

U.D.C. No. 533.661 : 533.6.071.4

Technical Note No. Aero 2378

May, 1955

ROYAL AIRCRAFT ESTABLISHMENT

Wind Tunnel Tests on a 6 ft Diameter Helicopter Rotor

by

T. B. Owen
R. Fail
and
R. C. W. Eyre

SUMMARY

Thrust, torque and flapping angle have been measured on a 6 ft diameter rotor over a range of blade angle, shaft inclination and tip speed ratio for comparison with the 12 ft diameter rotor previously tested in the 24 ft tunnel. In addition to tests in the 24 ft tunnel, the 6 ft diameter rotor was also tested in the No.2 11½ ft tunnel to investigate tunnel constraint. Brief investigations were made of support interference and blade twisting.

There are small discrepancies both as regards tunnel corrections and as regards the comparison of the 6 ft and 12 ft diameter rotors in the installed operating range. Possible reasons are discussed but small unexplained discrepancies remain. Blade stalling has larger effects on the 6ft diameter rotor but owing to the progressive nature of the phenomenon it is not possible to define any precise limits to the ranges of validity of the results on the two rotors.

N.L.L. No. 8, 71, 87, 125, 140, 124, 141, 89, 110, 90, 108, 76, 82, 122, 131

LIST OF CONTENTS

LIST OF TABLES

LIST OF ILLUSTRATIONS

1 Introduction

It was intended to test both a 6 ft diameter rotor and a 12 ft diameter rotor in the 24 ft tunnel in order to assess the reliability of model tests in a wind tunnel. The 12 ft rotor results are reported in Ref.1; the 6 ft rotor has now been tested, both in the 24 ft tunnel and the No.2 11½ ft tunnel. The intention was to obtain a method of tunnel corrections from the 6 ft rotor tests in the two tunnels, and then to compare the corrected results on the 6 ft and 12 ft rotors. In the course of examining possible reasons for discrepancies, blade twisting was measured under certain operating conditions and brief measurements were made of the interference effect of the supporting structure in the static thrust condition. The experiments were made at various times between January and April 1954.

2 Description of rotor and test equipment

2.1 Rotor

The 6 ft diameter rotor (Fig.1) had three blades which were untwisted and of constant chord (3 in.) and section (NACA 0012). It was designed to be as nearly as possible, a half scale model of the 12 ft diameter rotor of Ref.1. A detailed comparison of the two rotors is given in Table II. The blades of both rotors were constructed in the same way, and of the same materials, the method of construction being intended to locate the C.G. of the blades on the quarter chord line. Table II shows that the 6 ft blades were relatively 2.4% heavier and 7.7% stiffer in torsion than the 12 ft blades.

The hub incorporated flapping and drag hinges, with solid friction damping on the latter. The ball bearing flapping hinges on the 12 ft rotor wore very rapidly; in the 6 ft rotor, roller bearings of relatively greater load capacity were used and showed no signs of wear after the tests described in this note. It was not found possible to scale the 12 ft rotor hub down to half size and Table II shows that the overall diameter of the 6 ft rotor hub, including blade root fittings, was 17% of the rotor diameter compared with 13.9% for the 12 ft rotor.

2.2 Test equipment

The rotor was driven by a 6 H.P. electric motor which required a reduction gear box with a ratio of 13.86. The torque was measured in the same way as on the 12 ft rotor, by mounting the motor and gear box as a unit on ball bearings inside an outer casing and restraining this unit by means of a radial steel spring fitted with strain gauges. An A.C. strain gauge bridge was used. The gear box diameter was larger than desirable because of the large ratio and the diameter of the outer casing was 11.5% of the rotor diameter compared with 7.8% for the 12 ft rotor.

Rotational speed of the rotor was measured by means of a "condenser bridge" operated by means of a commutator on the rotor shaft. Longitudinal flapping angles were determined from photographs of the disk taken from the side of the tunnel with a remotely controlled F/24 camera.

2.3 Installation on wind tunnel balances

The 6 ft diameter rotor was mounted on the upper balances of the 24 ft and 11½ ft wind tunnels as shown in Figs.2 and 4. In both cases the rotor was inverted relative to the normal operating conditions of a helicopter. Due to the weight of the blades, the coning angles are larger by about 0.1°

than would be the case with the rotor operating normally. This is little more than the accuracy of the measurements. The 12 ft rotor was mounted on the lower balance of the 24 ft tunnel and was not inverted.

Experience with the 12 ft rotor had shown the danger of very severe vibration due to "ground resonance" if the rotational speed of the rotor coincided with a natural frequency of the supporting structure. Before running the 6 ft rotor, the main structural frequencies of the supporting systems were therefore investigated briefly with a hand held vibrograph. It was found that the appropriate modes had frequencies around 6 c.p.s. compared with about 18 r.p.s. of the rotor. The resonance while passing through the critical speed was noticeable but quite acceptable. The forward speed was limited by vibration only at $\theta_0 = 12^\circ$ and shaft inclinations of 0° and 5°, otherwise the rotor ran very smoothly at 1100 r.p.m.

3 Method of test and presentation of results

The tests were made at 1100 r.p.m.* giving a tip speed of 346 ft/sec and a tip Reynold's number of 0.54×10^6, with the exception of the higher blade angles in the static condition when rotational speed was limited by the power available (Table III). With fixed values of blade angle and shaft inclination, readings of lift, drag, and torque were taken at wind speeds of 36, 70, 106 and 140 ft/sec, corresponding to approximate tip speed ratios of 0.1, 0.2, 0.3 and 0.4. Photographs were also taken in each case from which the flapping angles were measured. The lift and drag readings were corrected for the tare lifts and drags of the rig without rotor and for the rotor weight, and resolved to give thrust and force in the plane of the disk. A nomenclature diagram is given in Fig.5. The thrust and torque coefficients and flapping angles were plotted against tip speed ratio and values read off at standard tip speed ratios. This procedure was repeated for shaft inclinations of 0°, 5°, 10°, 15°, 20° and 25° at blade angles of 4°, 8° and 12°.

Some extra tests over a wider range of blade angle were made to establish the rotor characteristics in the static thrust condition.

The flapping angles quoted throughout the present note are defined by the following equation:

$$\beta = a_0 - a_1 \cos\psi - b_1 \sin\psi$$

where β is the blade flapping angle measured from the no feathering plane (Fig.5) when the position of the blade in azimuth is ψ measured from the downwind position, positive in the direction of rotation, and a_1 is the longitudinal flapping angle or backward tilt of the disk.

The results of the tests on the 6 ft rotor are given in Tables III to VI. In the figures, measurements on the 12 ft rotor of Ref.1 and calculated curves (para 4) have been plotted for comparison where appropriate.

---

* The 12 ft diameter rotor was tested at 600 r.p.m.

The 6 ft rotor was designed to run at 1200 r.p.m. but the motor power supply was remote from the 24 ft wind tunnel and the resistance of the control leads made it impossible to achieve 1200 r.p.m. with a reasonable control margin. The speed was therefore reduced to 1100 r.p.m. and the same speed was used in the 11½ ft tunnel.

As explained in para 7.1 it has been found best to make the comparisons between the two rotors and theory by presenting the results as functions of disk incidence. (Shaft inclination was used in Ref.1).

All of the results have been corrected for tunnel constraint (para 6) and support interference (para 5).

4 Formulae given by theory

The calculated results quoted in this note are based on those given in Ref.2. The following formulae were used:

Thrust coefficient

$$C_T = \frac{\sigma a}{4}\left[\frac{2}{3}\theta_o\left(\frac{1 - \mu^2 + 2.25\,\mu^4}{1 + 1.5\,\mu^2}\right) - \lambda\left(\frac{1 - 0.5\,\mu^2}{1 + 1.5\,\mu^2}\right)\right]$$

Torque coefficient

$$C_Q = \frac{\sigma\delta}{8}(1 + \mu^2) + 1.1\,\frac{\sigma a}{4}\lambda\left[\frac{2}{3}\theta_o\left(\frac{1 - 0.5\,\mu^2}{1 + 1.5\,\mu^2}\right) - \lambda\left(\frac{1 + 0.5\,\mu^2}{1 + 1.5\,\mu^2}\right)\right]$$

Longitudinal flapping angle

$$a_1 = \frac{8}{3}\mu\left(\frac{\theta_o - 0.75\lambda}{1 + 1.5\,\mu^2}\right)$$

Disk incidence

$$\tan i_d = \frac{\lambda}{\mu} - \frac{C_T}{2\mu\left(\mu^2 + \lambda^2\right)^{\frac{1}{2}}}$$

For zero wind speed these formulae reduce to:

$$C_T = \frac{\sigma a}{4}\left(\frac{2}{3}\theta_o - \lambda\right)$$

$$C_Q = \frac{\sigma\delta}{8} + 1.1\,\frac{\sigma a}{4}\lambda\left(\frac{2}{3}\theta_o - \lambda\right)$$

$$2\lambda^2 = C_T$$

In these formulae

θ_o = blade angle in radians

σ = solidity (= 0.0796)

μ = tip speed ratio $\dfrac{V \cos i_S}{\Omega R}$

$\lambda = \dfrac{\mu}{\Omega R}$

a = lift curve slope per radian

δ = mean blade profile drag coefficient.

The above theory is approximate; it assumes uniform induced velocity (except that the factor of 1.1 applied to the induced torque coefficient makes some allowance for non-uniformity of induced velocity) and it makes no allowance for tip loss. The appropriate values for a and δ have been deduced from the measurements of thrust and torque in the static condition. A value of 4.9 for a has been used; Fig.6 shows that this gives calculated thrusts which are in agreement with the measured thrusts of both 6 ft and 12 ft rotors except near the stall. The small differences in static torque (Fig.7(a)) result in separate curves of δ for the two rotors (Fig.7(b)). These curves have been used in calculating the torques with forward speed applied, i.e. for the purpose of the calculations the discrepancy in torque is assumed to be due to differences in the profile drag coefficients of the blades. This discrepancy in torque may alternatively be attributed to a difference in the distribution of induced velocity between the two rotors. Thus, applying factors to the induced torque coefficient of 1.17 for the 6 ft rotor and 1.10 for the 12 ft rotor brings the profile drag curves of Fig.7(b) into close agreement. An increase in the profile drag coefficient of the blades is to be expected at the lower Reynold's number of the 6 ft rotor[4]. A change in the distribution of induced velocity seems less likely but this explanation is supported by the shapes of the curves of δ in Fig.7(b).

Analysis of the static thrust data by means of strip theory, which allows for the distribution of induced velocity and for tip losses, gives a value for the two dimensional lift curve slope of 5.4; this value agrees reasonably with the data of Ref.4. Relative to the value of 4.9 used in the approximate theory, about $^2/_3$ of the difference is due to non-uniformity of induced velocity and the remainder to tip losses.

5 Static thrust and torque

The static thrust measurements on the 6 ft rotor were made in the 24 ft tunnel with the rotor axis horizontal and a tarpaulin hung over the tunnel fan to prevent flow round the tunnel. The results are given in Table III and plotted in Figs.6 and 7.

Interference of the supporting structure was investigated in the static thrust condition by attaching dummy support tubes and a flat collar round the motor casing, as shown in Fig.3. The dummy support tubes reduced the thrust by 1.3% and increased the torque by less than 0.5%. The effects of the collar were too small to be measured. It is assumed that the same corrections will apply with forward speed and all of the thrust measurements given in this note have been increased by 1.3% to correct for support interference.

In Ref.1 the thrust measurements on the 12 ft rotor are increased by 4.5% to correct for support interference, on the basis of an experiment in which the loss of thrust due to a plank of flat section under a rotor was measured[6]. The present tests indicate that this estimate of the correction is excessive, for two reasons: the effect of a blockage near the centre of the rotor is negligible, and the effect of round tubes is less than that of a flat surface. Using the new data it is estimated that the loss of thrust due to the supporting structure of the 12 ft rotor was 0.5% with the rotor axis vertical and 2.2% with the axis horizontal. In the experiments the difference in thrust in the two cases was less than the accuracy of the measurements. In the present note, therefore, a correction of 1.3% has been applied to the thrusts of the 12 ft rotor.

Fig.6 shows that the static thrusts of the 6 ft and 12 ft rotors are in good agreement except near the stall. The 6 ft rotor stalls at a blade angle about 1.5° less than that of the 12 ft rotor.

The static torques of the two rotors are in fairly good agreement as shown in Fig.7(a). The small differences have been discussed in para 4.

6 Wind tunnel corrections

It was found that, at the same geometric shaft inclinations, the 6 ft rotor gave values for thrust and torque about 5% higher in the $11\frac{1}{2}$ ft tunnel than in the 24 ft tunnel. Tunnel constraint corrections were then applied as follows:

(a) In the 24 ft (open jet) tunnel the effective shaft inclination (or disk incidence) is greater than the geometric inclination by an amount:

$$\Delta i = \frac{1}{8} \frac{S}{C} C_L \text{ radians.}$$

(b) In the $11\frac{1}{2}$ ft (closed) tunnel the effective inclination is less than the geometric inclination by an amount:

$$\Delta i = \frac{1}{8.68} \frac{S}{C} C_L \text{ radians}$$

where S is the disk area, C is the area of the tunnel cross section, and C_L is the overall lift coefficient:

$$C_L = \frac{2C_T}{\mu^2 \sec^2 i_S}$$

Results obtained in the two tunnels, corrected in this way, are compared in Figs.8, 9 and 10. It will be seen that the discrepancies in thrust are closely accounted for by the tunnel constraint. The discrepancies in torque are not removed by any such incidence correction. This implies a change in the distribution of induced velocity due to tunnel interference. The flapping angles are generally about the same in the two tunnels except at $\theta_0 = 12^\circ$ when the flapping is about 0.4° less in the $11\frac{1}{2}$ ft tunnel.

The above corrections to incidence have been applied throughout the rest of this note, but no attempt has been made to apply any empirical correction to the torque.

7 Comparison of 6 ft and 12 ft rotors and theory

7.1 Flapping and coning angles

Fig.13 shows that the measured flapping angles are larger than those calculated, and increase more rapidly with blade angle and tip speed ratio than the approximate theory indicates. Judging from previous tests[1,5], the approximate theory does not predict flapping angles accurately. The comparison between the 12 ft and 6 ft rotors shows that the 6 ft rotor has flapping angles about 0.5° greater than the 12 ft rotor. An empirical tunnel correction based on the data of Figs.8-10 increases the disagreement. This discrepancy between the tests on the two rotors is serious as no reason for it has been found.

The thrust and torque of a rotor are determined by the incidence of the disk; the shaft inclination is of little significance. The results are therefore presented as functions of the disk incidence, which removes any discrepancies in thrust and torque due to differences in flapping angle.

Coning angles of the 6 ft rotor measured in the 24 ft tunnel are given in Tables IV-VI. These results can be well represented by:

$$a_o = 5.4\, C_T \quad \text{radians}$$

which is in good agreement with the relation obtained for the 12 ft rotor.

7.2 Thrust coefficients

Thrust coefficients measured for the 6 ft and 12 ft rotors in the 24 ft tunnel are shown in Fig.11. These results are corrected for support interference (Section 5) and tunnel constraint (Section 6). Calculated values are also given for comparison.

Under conditions remote from those which cause stalling of the retreating blade, (i.e. at low values of the blade angle and tip speed ratio and high values of the disk incidence) the measurements are in fair agreement with the calculations, although the thrusts measured for the 6 ft rotor are higher than those for the 12 ft rotor by an amount corresponding very roughly to 0.5° of blade angle or 1.5° of disk incidence. This discrepancy cannot be satisfactorily explained. Blade twisting is discussed in this connection in para 8.

The onset of stalling of the retreating blade is shown by the divergence of the thrust from the calculated value at high values of the blade angle and tip speed ratio and low values of the disk incidence. As already pointed out in Ref.1, the effects of stalling are progressive in character so that it is not possible to deduce a simple stalling criterion. Similarly, it is not possible to say with any certainty that the stall occurs "earlier" on the 6 ft rotor, although the loss of thrust is certainly greater on the 6 ft rotor than on the 12 ft rotor under conditions where appreciable blade stalling is obviously occurring.

7.3 Torque coefficients

Torque coefficients are plotted in Fig.12. The disk incidence is corrected for tunnel constraint (para 6). Calculated curves (para 4) are shown for comparison.

Except under conditions causing blade stalling the measurements are in fair agreement with the calculations. The 6 ft rotor generally has a higher torque than the 12 ft rotor. This was also the case in the static condition and the reasons are discussed in para 4. The same remarks apply to the results with forward speed applied.

Stalling of the retreating blade is shown by an increase in the torque above the calculated values at high values of the tip speed ratio and blade angle and low values of the disk incidence. Under conditions where an appreciable part of the retreating blade is obviously stalled, the torque of the 6 ft rotor is much higher than that of the 12 ft rotor, but, as in the case of the thrust, it is not possible to say whether or not the stall begins to have significant effects at different conditions for the two rotors.

7.4 Forces in the plane of the disk

Forces in the plane of the disk are small and therefore of little practical importance. Results obtained on the 6 ft rotor in the 24 ft and 11½ ft tunnels are plotted in Fig.14. It is of interest that the force in the plane of the disk is negative (i.e. directed, forward instead of backward) in conditions in which a stall would be expected on the retreating blade. This phenomenon was noted and discussed in Ref.1. The present results are more complete and show less scatter.

8 Blade twisting

Blade twisting was measured on the 6 ft rotor in the 24 ft tunnel by fitting a small mirror in the leading edge of one blade, near the tip, and observing the position of the reflection of a point source of light.

Under static conditions tests were made at blade angles of 4°, 8° and 12°. The results are shown in Fig.15. The twisting is small and negative and varies rather erratically.

Tests were also made at $\theta_0 = 8^\circ$, $i_S = 20^\circ$ and $\mu = 0.3$ (which gives roughly zero thrust). The results are shown in Fig.16. The twisting is again negative and is considerably larger than in the static case; there is some variation around the disk.

These results can be explained as follows. Blade twisting is caused in two ways:

(1) The so-called "propeller moment", due to centrifugal forces on the blade, tends to bring the blade chord lines into the plane of rotation. For the present models the equations given in Ref.3 reduce to:

$$\Delta\theta_0 = -\frac{\Omega^2 I \sin 2\theta}{4gK}(R - R_0)^2 \text{ radians}$$

(ignoring the moment of inertia of the blade section about its major axis) where $\Delta\theta_0$ is the twist of the blade at the tip*.

---

* All values of the twist (measured and calculated) quoted refer to the tip of the blade. The twist at 0.7R is about 80-85% of the value at the tip.

(2) Lift on the blades tends to increase the blade angle if the C.P. is ahead of the C.G. For parabolic lift distribution:

$$\Delta\theta_o = \frac{\rho\Omega^2 \bar{C}_L \times c^2}{2K}\left(\frac{R^4}{4} - \frac{R^3 R_o}{3} + \frac{R_o^4}{12}\right) \text{ radians}$$

where x is the distance of the C.P. ahead of the C.G. (in terms of the blade chord) and $\bar{C}_L$ is the blade lift coefficient. It is difficult to measure accurately the blade C.G. position without spoiling the blades for further rotor tests and the measurements given in Table II must therefore be regarded as approximate. Values for the C.P. position are given in Ref.4 and quoted in Table II. It appears that the C.P. is about 2½% c ahead of the C.G. on the 6 ft rotor blades and about 1% ahead on the 12 ft rotor blades.

Values of the twist calculated for the 6 ft rotor in the static condition at 1100 r.p.m. are given in the following table:

θ_o°	Aerodynamic Twist (°)	C.P. Twist (°)	Total Twist (°)
4	+0.12	-0.22	-0.10
8	+0.32	-0.44	-0.12
12	+0.56	-0.65	-0.09

The twists due to the aerodynamic and centrifugal forces are opposite in sign and of the same order of magnitude. The resultant twist is small and negative and is therefore in qualitative agreement at least with the measurements. The irregular variations with speed in the measurements may be due to scale effects on the C.P. position.

At $\theta_o = 8°$, $i_S = 20°$ and $\mu = 0.3$ the thrust (and therefore the mean lift on the blades) is small. The dotted line in Fig.16(b) is therefore calculated assuming no aerodynamic twist. It will be seen that the measured points lie below the line (i.e. the measured twist is more negative than the calculated value). There is probably a distribution of lift on the blades, producing twist, although the overall thrust is nearly zero.

It has already been pointed out that it is difficult to estimate accurately the aerodynamic twisting; the available data indicate that the 12 ft rotor was more closely mass balanced than the 6 ft rotor, and would therefore be expected to twist slightly less positively. On the other hand, there is no reason to suppose that the twisting due to centrifugal forces was different on the two rotors. The discrepancy in thrust (para 7.2) exists at zero thrust and therefore cannot be attributed to differences in blade twisting.

9 Conclusions

Over the normal operating range, there are small unexplained discrepancies between the measurements made on the 6 ft and 12 ft diameter rotors. Blade stalling has larger effects on the 6 ft rotor than on the 12 ft rotor, though its onset may not be earlier.

The tests on the 6 ft rotor in the 24 ft and 11½ ft tunnels indicate that the usual tunnel constraint correction to incidence is satisfactory so far as thrust is concerned. Higher torques were measured in the smaller (closed) tunnel. This discrepancy is not removed by the usual constraint correction; this implies a redistribution of the induced velocity.

It is shown that, for the present models, blade twisting of the order of 0.5° occurs due to aerodynamic and centrifugal forces, but that blade twisting is unlikely to be responsible for the discrepancies mentioned above.

REFERENCES

No.	Author	Title, etc.
1	H.B. Squire, R.A. Fail and R.C.W. Eyre	Wind tunnel tests on a 12 ft diameter helicopter rotor R & M 2695 April, 1949
2	H.B. Squire and P. Sibbald	Tables of rotor characteristics RAE Tech Note No. Aero 1883 April, 1947
3	P.R. Payne	A method of rapidly estimating propeller moment Journal of Royal Aeronautical Society No.520 Vol.58 April, 1954
4	E.N. Jacobs and A. Sherman	Airfoil section characteristics as affected by variations of the Reynolds Number NACA Report No.586 (1937)
5	P.A. Hufton and others	General investigation of the characteristics of the C.30 autogyro R & M 1859 1939
6	R.A. Fail and R.C.W. Eyre	Loss of static thrust due to a fixed surface under a helicopter rotor RAE Tech Note No. Aero 2008 July 1949 ARC 12585

TABLE I

List of symbols and leading dimensions

R	Radius of rotor	= 3.00 ft
R_o	Overall radius of hub (including blade root fitting)	
c	Chord of blades	= 0.25 ft
N	Number of blades	3
σ	Solidity of rotor $= \frac{Nc}{\pi R}$	= 0.0796
θ_o	Blade angle (deg or radn)	
i_{S_G}	Geometric shaft inclination (deg)	
Δi	Tunnel constraint correction on incidence (para 6)	
i_S	Shaft inclination corrected for tunnel constraint $= i_{S_G} + \Delta i$ (deg)	
a_1	Longitudinal flapping angle (deg)	
b_1	Lateral flapping angle (deg)	
i_d	Disk incidence corrected for tunnel constraint $= i_S - a_1$ (deg)	
a_o	Coning angle (deg)	
ψ	Blade position in azimuth (deg) measured from downwind position, positive in direction of rotation	
Ω	Angular velocity of rotor (radn/sec)	
V	Tunnel speed (ft/sec)	
u	Component velocity of air at rotor disk parallel to shaft	
T	Thrust (lb)	
Q	Torque (lb ft)	
F	Force in plane of disk (lb)	
ρ	Air density (slugs/ft^3)	
μ	Tip speed ratio $= \frac{V \cos i_S}{\Omega R}$	
λ	$\frac{u}{\Omega R}$	
a	Slope of lift curve of blade section per radian	

TABLE I (Contd)

δ	Mean profile drag coefficient of blade section
C_T	Thrust coefficient $= \dfrac{T}{\rho \Omega^2 R^2 \pi R^2}$
C_Q	Torque coefficient $= \dfrac{Q}{\rho \Omega^2 R^3 \pi R^2}$
C_F	Force coefficient $= \dfrac{F}{\rho \Omega^2 R^2 \pi R^2}$
$\overline{C_L}$	$\dfrac{6 C_T}{\sigma}$
η	Static thrust efficiency $= \dfrac{C_T^{3/2}}{\sqrt{2}\, C_Q}$
I	Moment of inertia of blade section about minor axis per foot run (lb ft)
K	Torsional rigidity of blades per foot run (lb ft^2/radn)

TABLE II

Details of 6 ft and 12 ft diameter rotors

Description	6 ft dia Rotor	12 ft dia Rotor
Motor casing radius	0.115 R	0.078 R
Flapping hinge radius	0.045 R	0.031 R
Drag hinge radius	0.090 R	0.066 R
Overall hub radius, including blade root fittings. (R_o)	0.170 R	0.139 R
Measured blade weight per foot run	0.282 lb	1.102 lb
Measured blade torsional rigidity per foot run. (K)	25.8 lb ft^2/radn	383 lb ft^2/radn
Calculated blade section inertia about minor axis per foot run. (I)	0.001044 lb ft	0.0167 lb ft
Measured blade c.g. position	0.264 c	0.250 c
Estimated c.p. position. (Ref.4)	0.239 c	0.240 c

TABLE III

Static coning, thrust and torque - 6 ft rotor

$\theta_o{}^o$	R.P.M.	$a_o{}^o$	$10^3 C_T$	$10^3 C_Q$	η
-1	1100	-0.05	-0.127	0.082	0.012
1.05	"	0.1	0.157	0.087	0.016
4	"	0.8	1.60	0.148	0.306
8	"	1.6	4.42	0.367	0.566
12	"	2.8	7.64	0.743	0.636
14	1000	3.3	9.15	0.977	0.634
16	900	3.8	10.67	1.217	0.641
17	850	4.05	10.99	1.431	0.569
18	800	3.8	10.70	1.810	0.432

TABLE IV

6 ft Rotor characteristics $\theta_o = 4^o$

24 ft Tunnel									$11\frac{1}{2}$ ft × $8\frac{1}{2}$ ft Tunnel								
μ	$i_{S_G}{}^o$	Δi^o	$i_S{}^o$	$a_1{}^o$	$a_o{}^o$	$i_d{}^o$	$10^3 C_T$	$10^3 C_Q$	μ	$i_{S_G}{}^o$	Δi^o	$i_S{}^o$	$a_1{}^o$	$a_o{}^o$	$i_d{}^o$	$10^3 C_T$	$10^3 C_Q$
0	-	-	-	0	0.8	-	1.60	0.148	0	-	-	-	0	-	-	-	-
0.1	0	0.3	0.3	1.7	1.05	-1.4	3.35	0.157	0.1	0	-1.35	-1.35	-	-	-	3.57	0.165
	5	0.25	5.25	1.6	0.9	3.65	2.65	0.149		5	-1.1	3.9	1.45	-	2.45	2.87	0.165
	10	0.2	10.2	1.0	0.65	9.2	2.05	0.144		10	-0.8	9.2	1.1	-	8.1	2.25	0.167
	15	0.1	15.1	0.9	0.6	14.2	1.48	0.138		15	-0.55	14.45	0.8	-	13.65	1.59	0.158
	20	0.05	20.05	0.7	0.5	19.35	0.82	0.119		20	-0.3	19.7	0.6	-	19.1	0.91	0.134
	25	0	25.0	0.5	0.25	24.5	0.18	0.091		25	-0.05	24.95	0.4	-	24.55	0.11	0.097
0.2	0	0.1	0.1	2.9	1.45	-2.8	4.54	0.111	0.2	0	-0.45	-0.45	-	-	-	4.75	0.130
	5	0.05	5.05	2.4	1.0	2.65	2.98	0.150		5	-0.3	4.7	2.55	-	2.15	3.17	0.164
	10	0.05	10.05	1.8	0.45	8.25	1.39	0.136		10	-0.15	9.85	1.8	-	8.05	1.60	0.164
	15	0	15.0	1.5	0.10	13.5	-0.10	0.081		15	0	15.0	1.1	-	13.9	-0.09	0.098
	20	-0.05	19.95	0.6	-0.30	19.35	-1.82	-0.016		20	0.15	20.15	0.55	-	19.6	-1.79	-0.002
0.3	0	0.05	0.05	4.8	1.5	-4.75	5.25	0.022	0.3	0	-0.2	-0.2	4.75	-	-4.95	5.37	0.081
	5	0.05	5.05	3.6	0.95	1.45	2.97	0.137		5	-0.15	4.85	3.55	-	1.3	3.07	0.156
	10	0	10.0	2.3	0.15	7.7	0.42	0.110		10	0	10.0	2.25	-	7.75	0.59	0.132
	15	0	15.0	1.2	-0.35	13.8	-1.90	-0.017		15	0.1	15.1	0.9	-	14.2	-2.08	-0.011
0.4	5	0	5.0	4.8	0.85	0.2	3.02	0.112	0.4	5	-0.05	4.95	4.55	-	0.4	2.87	0.138
	10	0	10.0	2.2	0.05	7.8	0.25	0.063		10	0	10.0	2.25	-	7.75	-0.42	0.080

TABLE V

6 ft Rotor characteristics $\theta_o = 8^\circ$

24 ft Tunnel									$11\frac{1}{2}$ ft × $8\frac{1}{2}$ ft Tunnel								
μ	$i_{S_G}{}^\circ$	Δi°	$i_S{}^\circ$	$a_1{}^\circ$	$a_o{}^\circ$	$i_d{}^\circ$	$10^3 C_T$	$10^3 C_Q$	μ	$i_{S_G}{}^\circ$	Δi°	$i_S{}^\circ$	$a_1{}^\circ$	$a_o{}^\circ$	$i_d{}^\circ$	$10^3 C_T$	$10^3 C_Q$
0	-	-	-	0	1.6	-	4.42	0.367	0	-	-	-	0	-	-	-	-
0.1	0	0.55	0.55	3.2	1.85	-2.65	6.30	0.340	0.1	0	-2.55	-2.55	3.1	-	-5.65	6.74	0.347
	5	0.5	5.5	2.7	1.8	2.8	5.78	0.353		5	-2.3	2.7	2.9	-	-0.2	6.08	0.355
	10	0.45	10.45	2.3	1.65	8.15	5.32	0.361		10	-2.0	8.0	2.3	-	5.7	5.57	0.362
	15	0.4	15.4	2.0	1.65	13.4	4.74	0.360		15	-1.75	13.25	1.9	-	11.35	5.02	0.377
	20	0.35	20.35	1.75	1.4	18.6	4.16	0.348		20	-1.45	18.55	1.9	-	16.65	4.34	0.372
	25	0.25	25.25	1.6	1.3	23.65	3.50	0.332		25	-1.05	23.95	1.6	-	22.35	3.68	0.349
0.2	0	0.2	0.2	5.8	2.4	-5.6	8.05	0.316	0.2	0	-0.8	-0.8	5.9	-	-6.7	8.29	0.336
	5	0.15	5.15	5.5	2.1	-0.35	6.89	0.333		5	-0.65	4.35	5.15	-	-0.8	7.01	0.329
	10	0.1	10.1	4.3	1.65	5.8	5.41	0.348		10	-0.5	9.5	4.25	-	5.25	5.67	0.343
	15	0.1	15.1	3.65	1.35	11.45	3.88	0.334		15	-0.35	14.65	3.3	-	11.35	4.13	0.349
	20	0.05	20.05	2.95	0.85	17.1	2.36	0.275		20	-0.2	19.8	2.85	-	16.95	2.41	0.292
	25	0	25.0	2.7	-	22.3	0.59	0.145		25	-0.05	24.95	2.35	-	22.60	0.60	0.181
0.3	0	0.1	0.1	9.6	2.25	-9.5	8.85	0.430	0.3	0	-0.4	-0.4	9.5	-	-9.9	9.20	0.420
	5	0.05	5.05	8.0	1.95	-2.95	7.19	0.323		5	-0.3	4.7	7.95	-	-3.25	7.23	0.350
	10	0.05	10.05	6.2	1.5	3.85	4.91	0.319		10	-0.2	9.8	6.1	-	3.7	5.18	0.316
	15	0	15.0	4.9	0.65	10.1	2.61	0.284		15	-0.1	14.9	4.4	-	10.5	2.69	0.294
	20	0	20.0	3.45	-0.05	16.55	-0.08	0.107		20	0	20.0	3.25	-	16.75	-0.04	0.117
0.4	5	0.05	5.05	10.2	1.75	-5.15	7.71	0.402	0.4	5	-0.2	4.8	10.15	-	-5.35	7.56	0.406
	10	0	10.0	7.5	1.3	2.5	4.50	0.290		10	-0.1	9.9	7.7	-	2.2	4.63	0.299
	15	0	15.0	5.2	0.2	9.8	1.09	0.214		15	-0.05	14.95	5.1	-	9.85	1.23	0.213

Wt.2078.CP216.K3 - Printed in Great Britain

TABLE VI

6 ft rotor characteristics $\theta_o = 12^\circ$

24 ft Tunnel									$11\frac{1}{2}$ ft × $8\frac{1}{2}$ ft Tunnel								
μ	$i_{S_G}{}^\circ$	Δi°	$i_S{}^\circ$	$a_1{}^\circ$	$a_o{}^\circ$	$i_d{}^\circ$	$10^3 C_T$	$10^3 C_Q$	μ	$i_{S_G}{}^\circ$	Δi°	$i_S{}^\circ$	$a_1{}^\circ$	$a_o{}^\circ$	$i_d{}^\circ$	$10^3 C_T$	$10^3 C_Q$
0	-	-	-	0	2.8	-	7.64	0.743	0	-	-	-	0	-	-	-	-
0.1	0	0.8	0.8	5.2	2.75	-4.4	8.81	0.692	0.1	0	-3.55	-3.55	4.9	-	-8.45	9.28	0.736
	5	0.75	5.75	5.0	2.6	0.75	8.32	0.728		5	-3.3	1.7	5.0	-	-3.3	8.72	0.736
	10	0.7	10.7	4.7	2.65	6.0	8.00	0.677		10	-2.95	7.05	4.4	-	2.65	7.99	0.757
	15	0.65	15.65	3.6	2.8	12.05	7.90	0.674		15	-2.85	12.15	3.5	-	8.65	8.12	0.715
	20	0.6	20.6	3.4	2.65	17.2	7.45	0.678		20	-2.6	17.4	3.15	-	14.25	7.74	0.720
	25	0.5	25.5	3.2	2.4	22.3	6.84	0.680		25	-2.2	22.8	2.85	-	19.95	7.16	0.723
0.2	0	0.25	0.25	10.6	2.75	-10.35	10.31	0.910	0.2	0	-1.0	-1.0	10.5	-	-11.5	10.64	1.006
	5	0.2	5.2	9.4	2.65	-4.2	9.44	0.830		5	-0.9	4.1	9.1	-	-5.0	9.66	0.890
	10	0.2	10.2	9.3	2.4	0.9	8.12	0.756		10	-0.75	9.25	8.3	-	0.95	8.38	0.788
	15	0.15	15.15	6.8	2.4	8.35	7.43	0.630		15	-0.65	14.35	6.7	-	7.65	7.55	0.694
	20	0.1	20.1	5.6	2.0	14.5	6.20	0.616		20	-0.55	19.45	5.35	-	14.10	6.39	0.660
	25	0.1	25.1	4.9	1.65	20.2	4.62	0.576		25	-0.35	24.65	4.4	-	20.25	4.76	0.607
0.3	5	0.1	5.1	12.9	2.65	-7.8	10.14	0.915	0.3	5	-0.45	4.55	12.95	-	-8.4	10.39	0.982
	10	0.1	10.1	12.0	2.25	-1.9	8.44	0.790		10	-0.35	9.65	11.35	-	-1.75	8.74	0.825
	15	0.05	15.05	9.5	1.8	5.55	6.46	0.613		15	-0.25	14.75	9.15	-	5.6	6.72	0.684
	20	0.05	20.05	7.5	1.4	12.55	4.41	0.523		20	-0.15	19.85	6.8	-	13.05	4.57	0.561
	25	0	25.0	6.0	0.75	19.0	1.82	0.351		25	-0.05	24.95	5.3	-	19.65	1.77	0.365
0.4	15	0.05	15.05	11.2	1.75	3.85	5.88	0.615	0.4	15	-0.15	14.85	10.7	-	4.15	6.08	0.660
	20	0	20.0	8.2	0.85	11.8	2.45	0.410		20	-0.05	19.95	7.7	-	12.25	2.68	0.429
	25	0	25.0	6.0	0.05	19.0	-0.91	0.020		25	0	25.0	5.2	-	19.8	-1.17	-0.003

FIG.I.

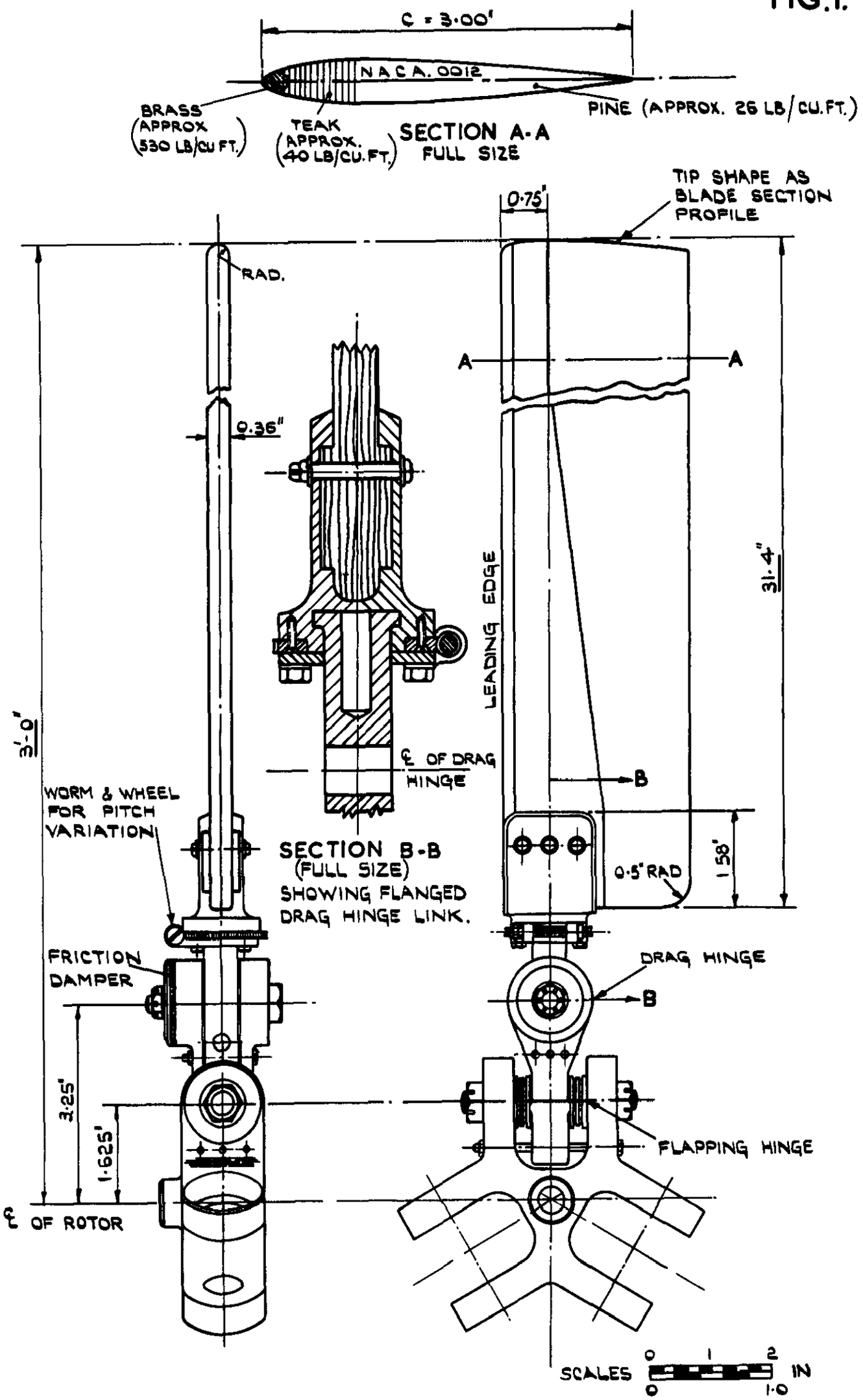

FIG.I. DETAILS OF 6 FT DIAMETER ROTOR.

FIG.2.

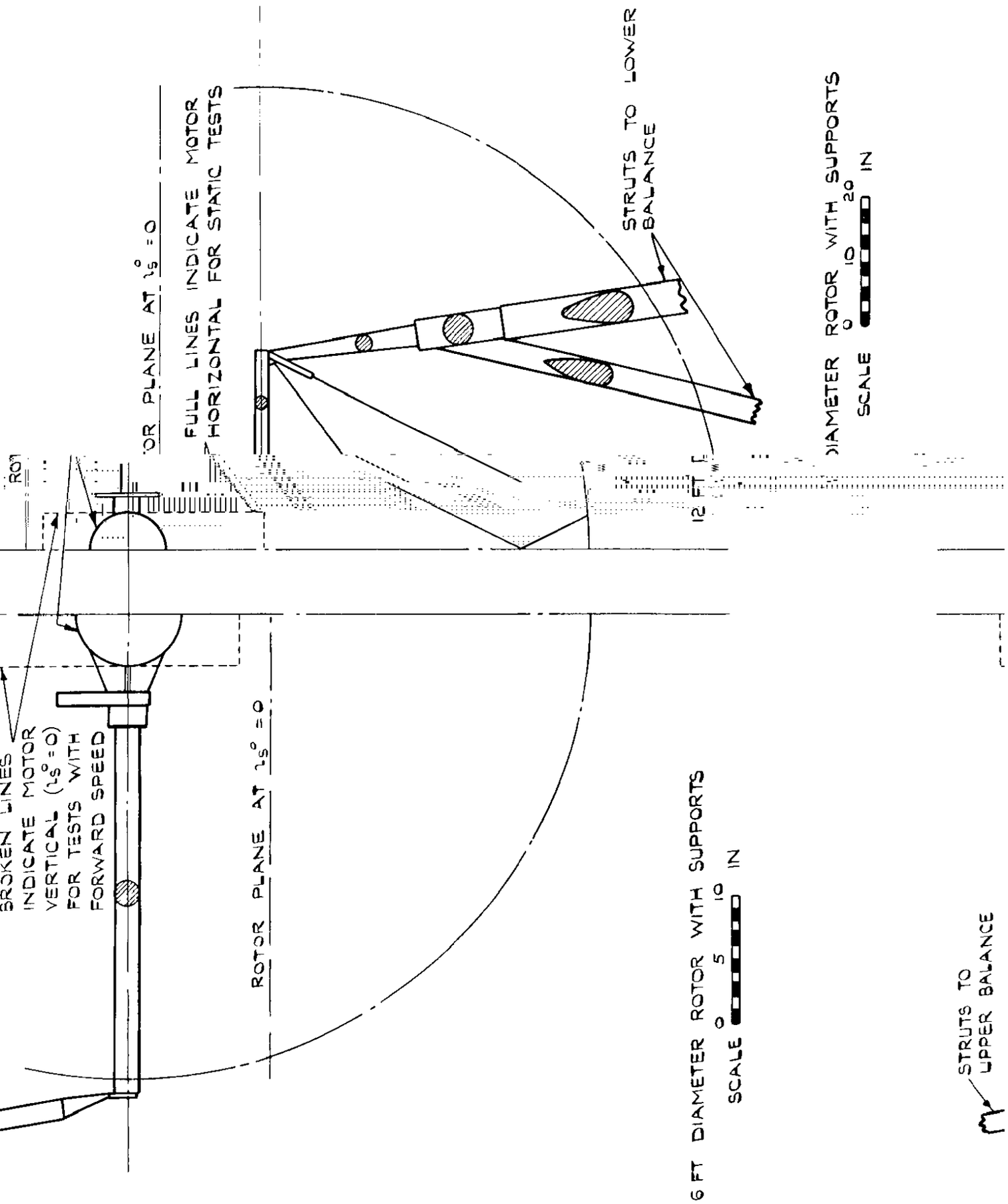

FIG. 2. COMPARISON OF SUPPORT RIGS--6 FT AND 12 FT DIAMETER ROTORS IN 24 FT TUNNEL.

FIG.3&4.

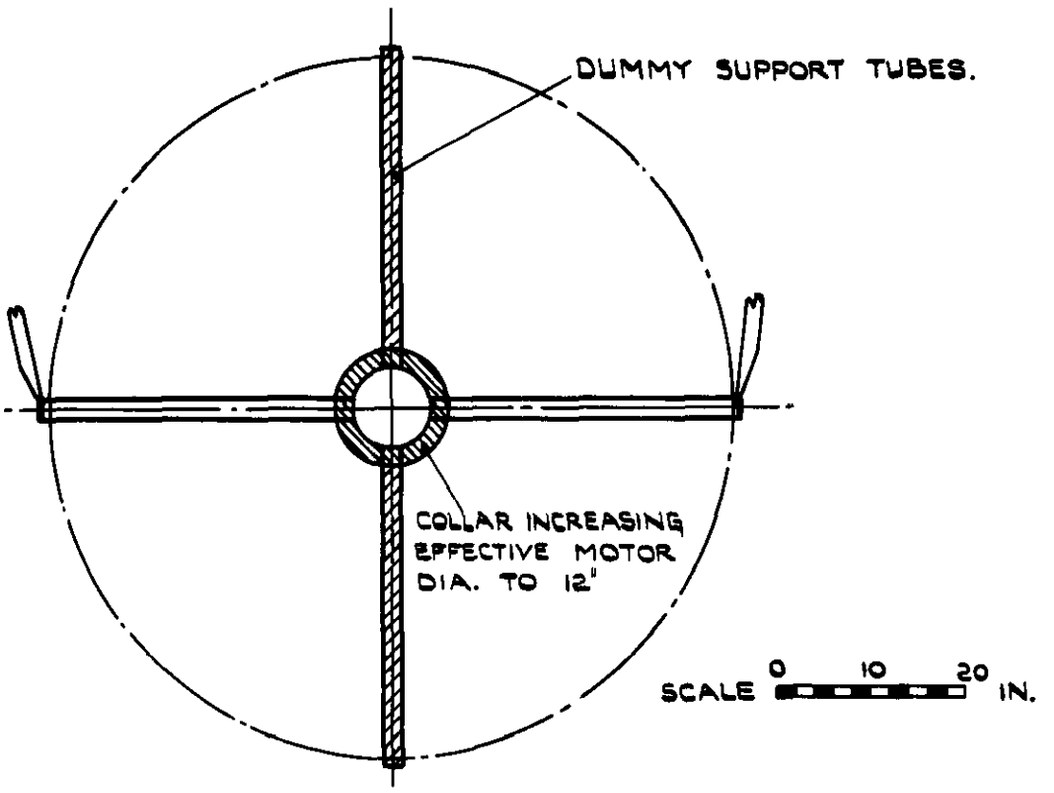

LOSS IN THRUST DUE TO DUMMY SUPPORT TUBES = 1·3%
LOSS IN THRUST DUE TO COLLAR - NEGLIGIBLE.

FIG.3. DUMMY SUPPORTS - 6 FT DIA. ROTOR STATIC TESTS IN 24 FT TUNNEL.

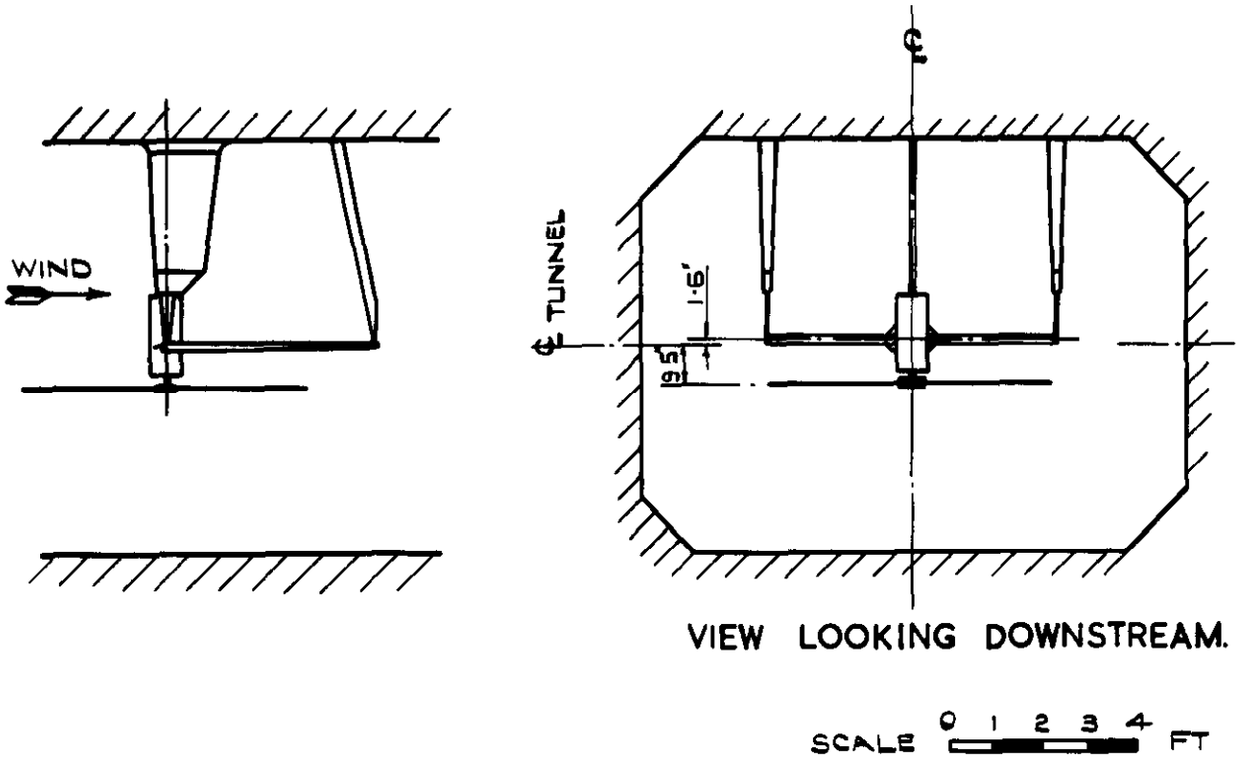

FIG. 4. ARRANGEMENT OF 6 FT DIAMETER ROTOR IN 11½ FT X 8½ FT TUNNEL.

FIG. 5.

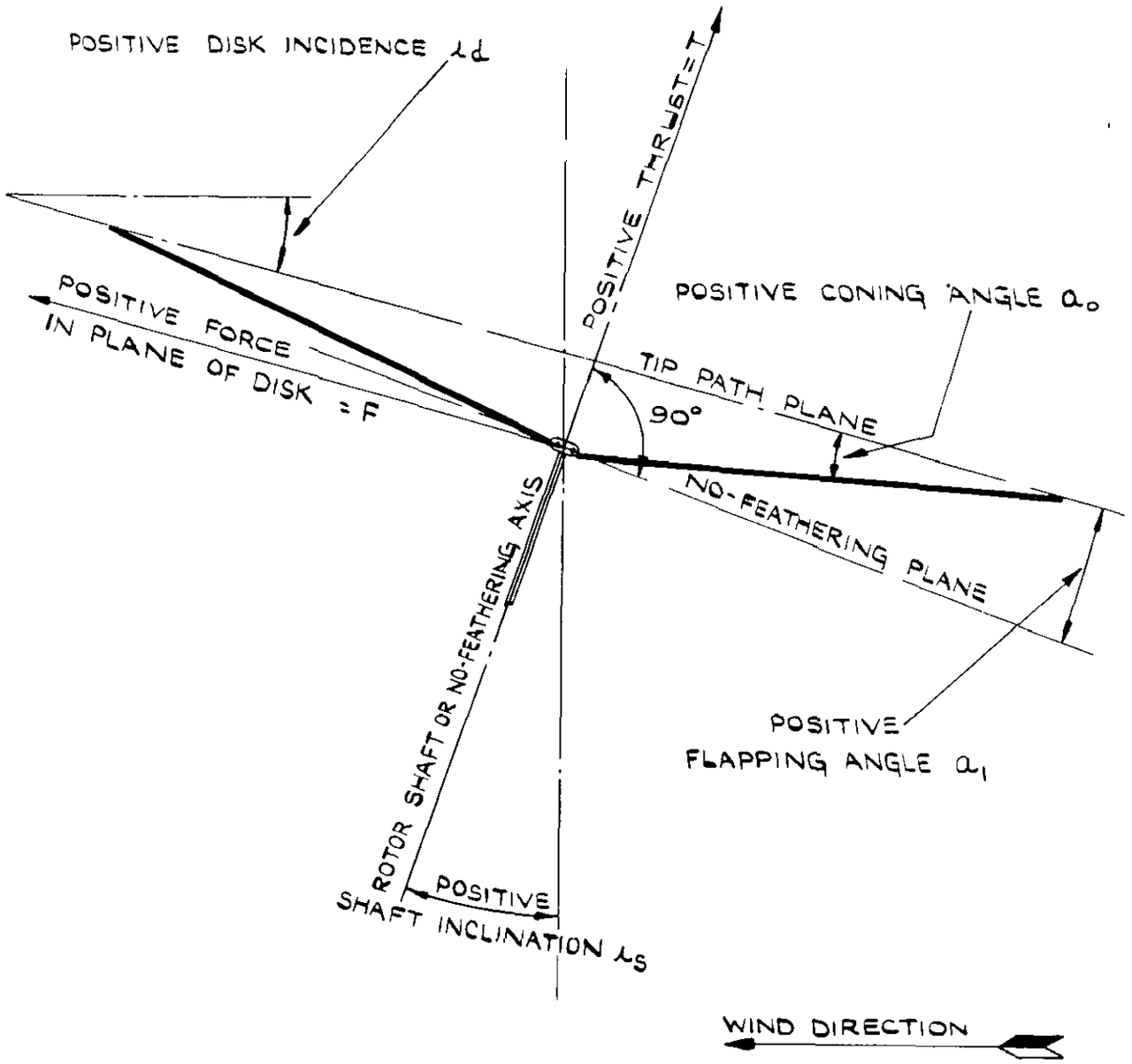

FIG. 5. NOMENCLATURE DIAGRAM.

FIG.6.

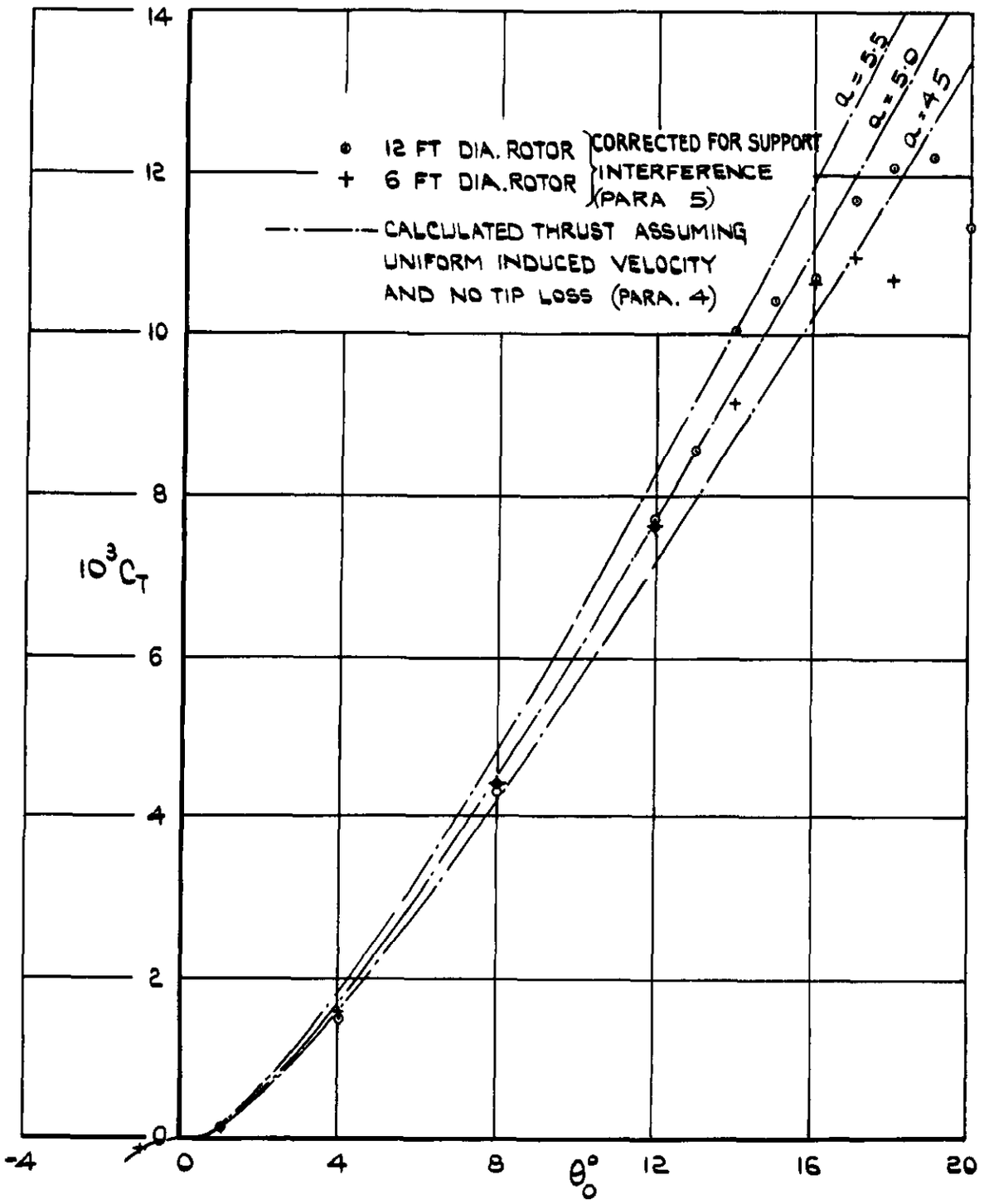

FIG. 6. STATIC THRUST COEFFICIENT.

FIG.7. (a & b)

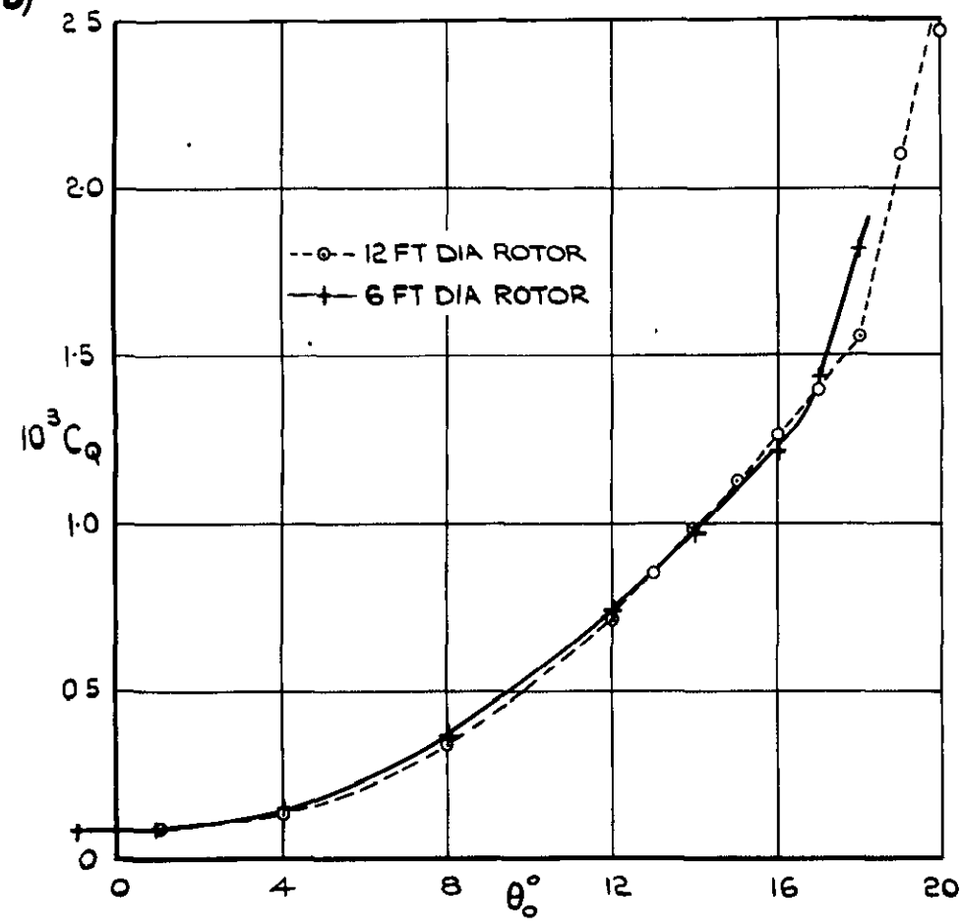

FIG. 7 (a) STATIC TORQUE COEFFICIENT.

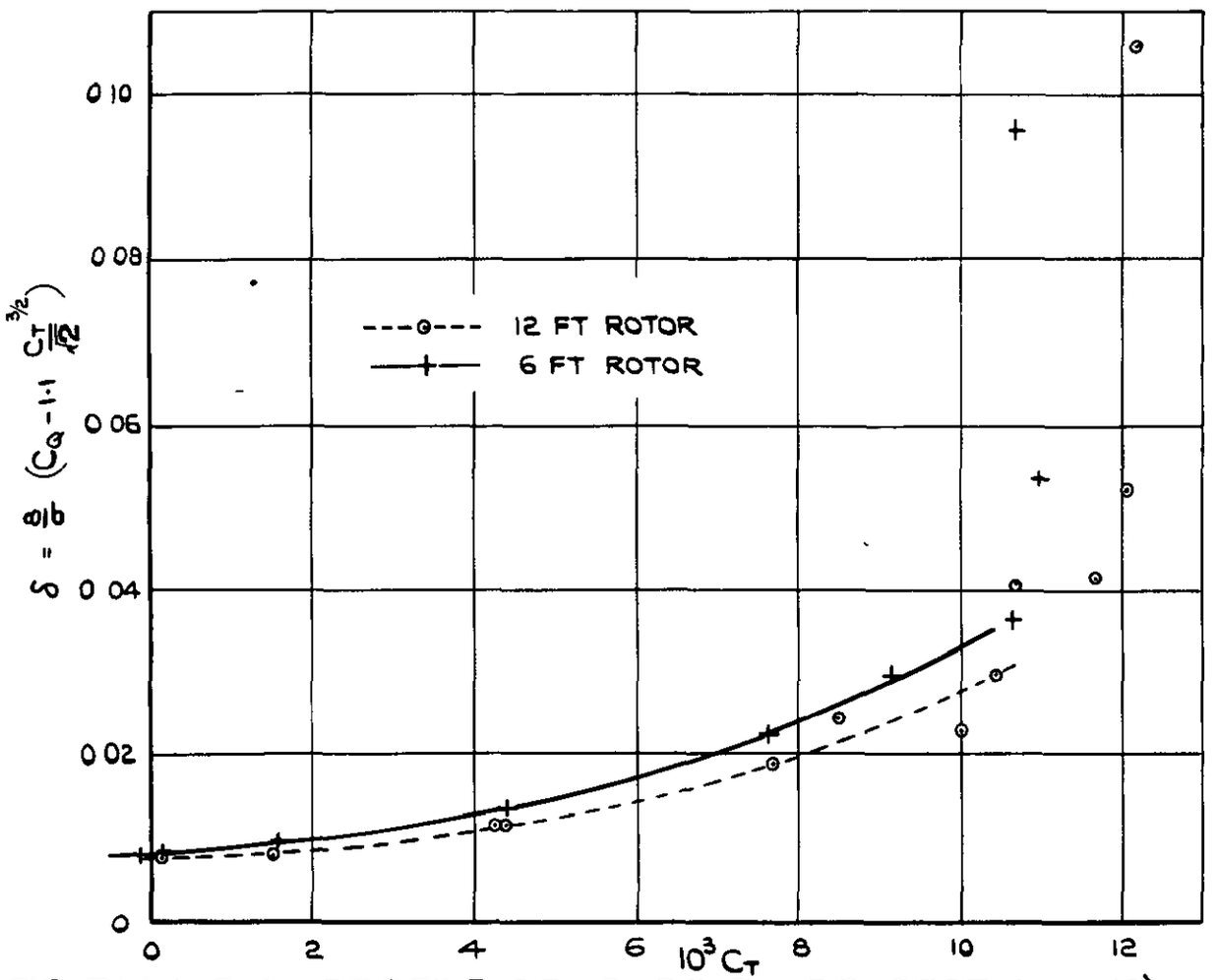

FIG. 7(b) MEAN PROFILE DRAG OF BLADE SECTION (δ) DEDUCED FROM MEASURED STATIC THRUST & TORQUE.

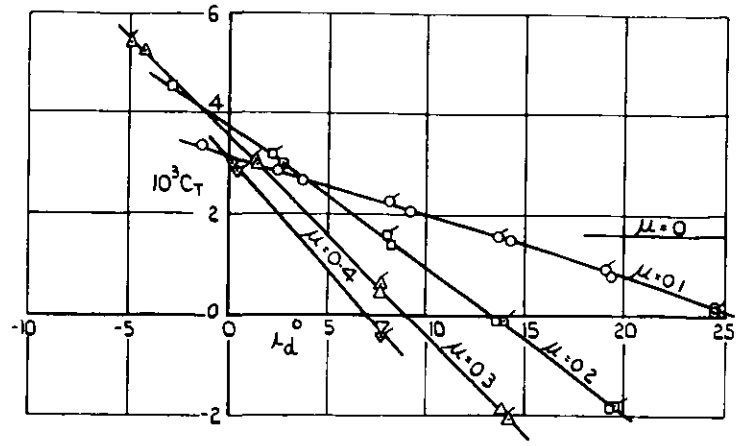

(a) THRUST

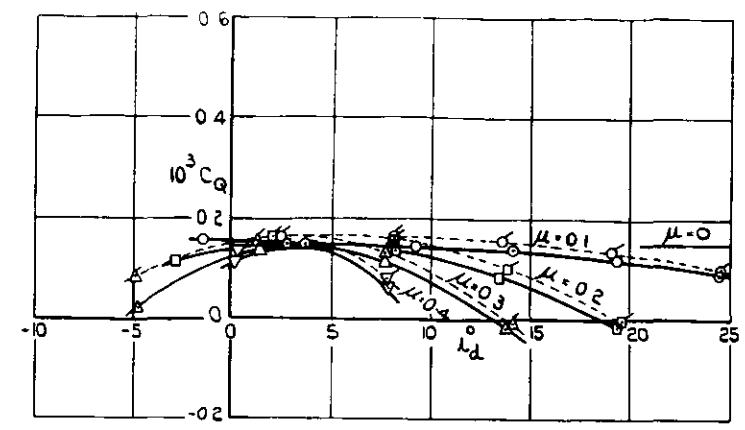

(b) TORQUE

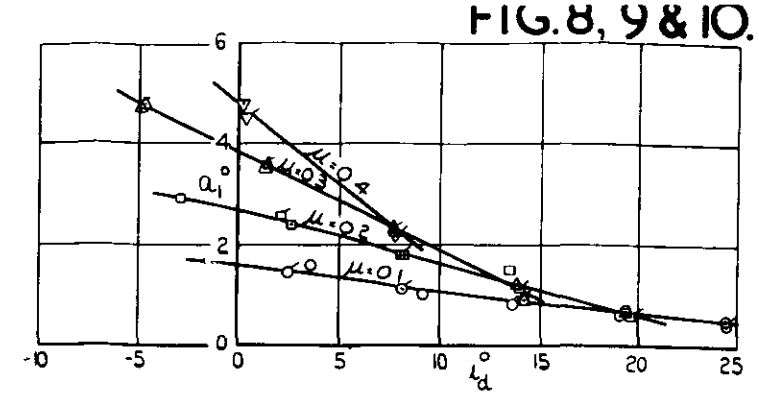

(c) FLAPPING ANGLE

FIG. 8. (a - c) 6 FT DIA. ROTOR - BLADE ANGLE $\theta_0 = 4^\circ$.

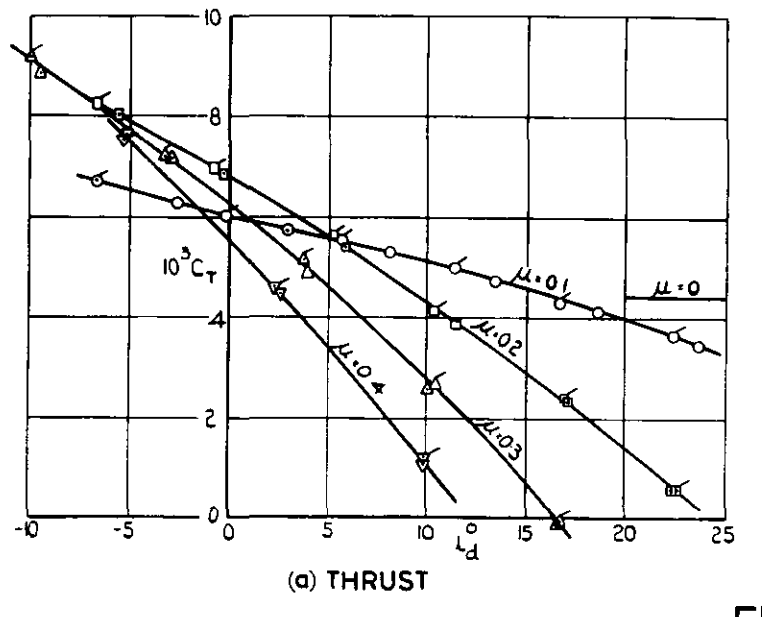

(a) THRUST

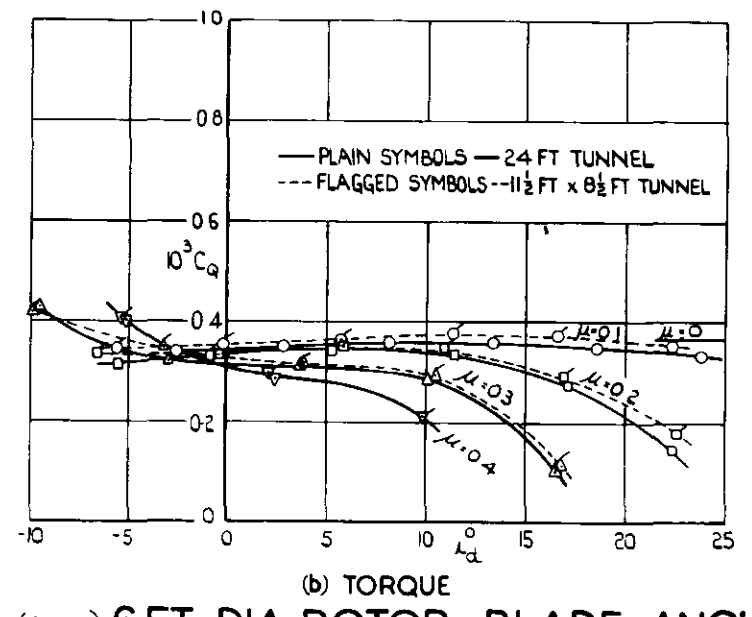

(b) TORQUE

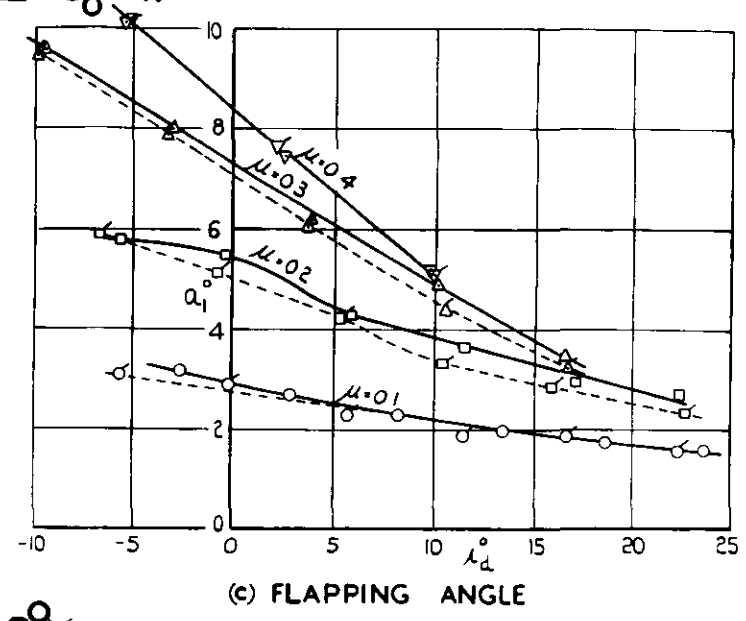

(c) FLAPPING ANGLE

FIG. 9. (a - c) 6 FT DIA. ROTOR - BLADE ANGLE $\theta_0 = 8^\circ$.

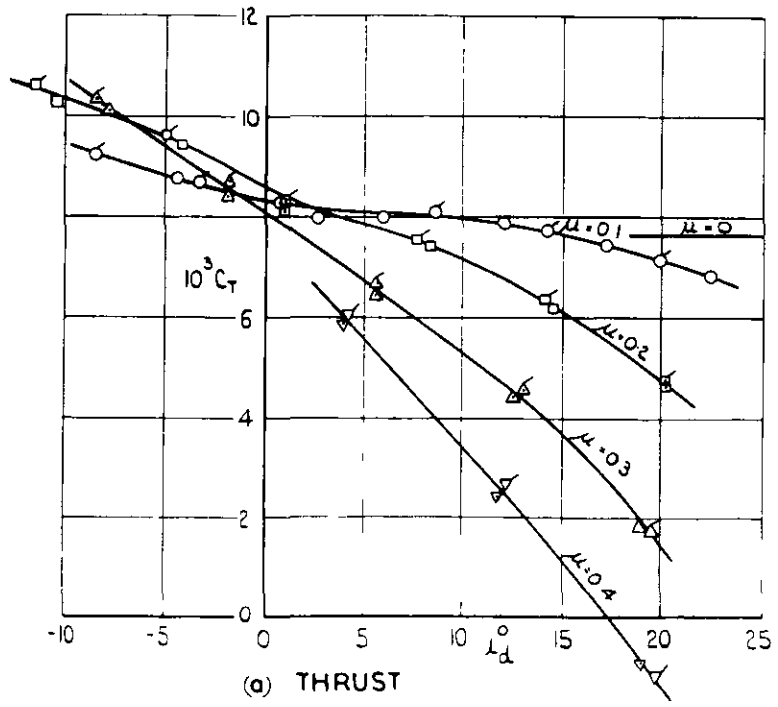

(a) THRUST

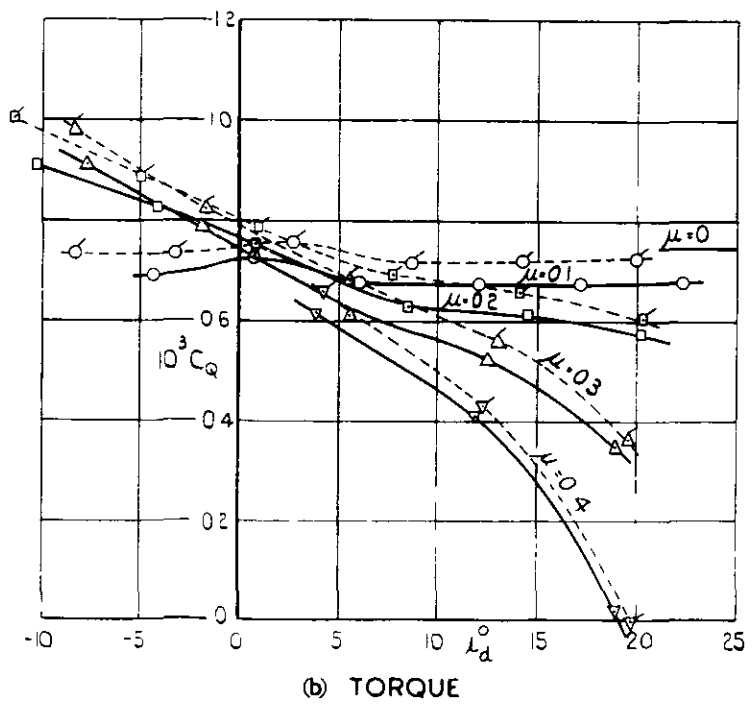

(b) TORQUE

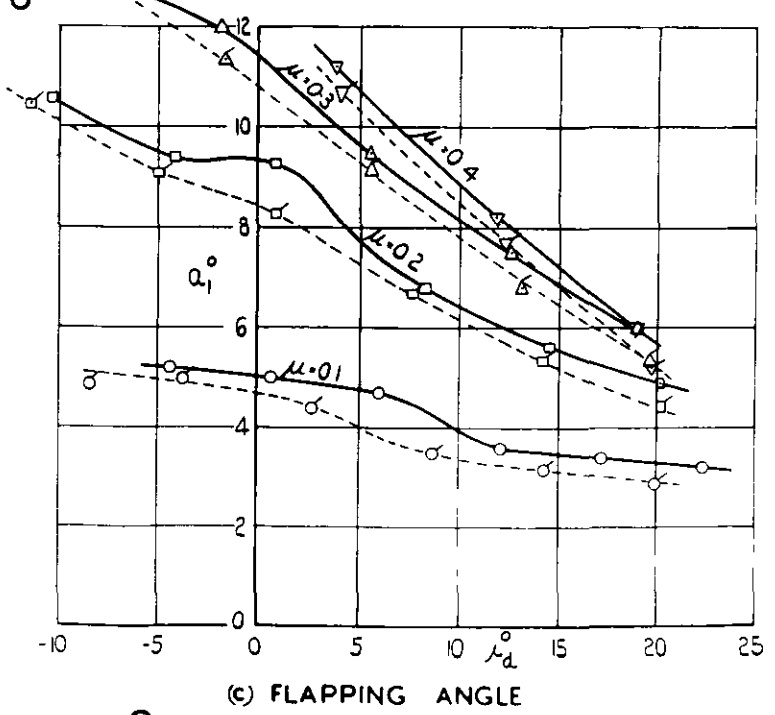

(c) FLAPPING ANGLE

FIG. 10. (a - c) 6 FT DIA ROTOR - BLADE ANGLE $\theta_0 = 12^\circ$.

FIG. 8, 9 & 10. COMPARISON OF 6 FT DIA. ROTOR CHARACTERISTICS MEASURED IN 24 FT TUNNEL AND 11½ FT x 8½ FT TUNNEL.

FIG.11. (a & b)

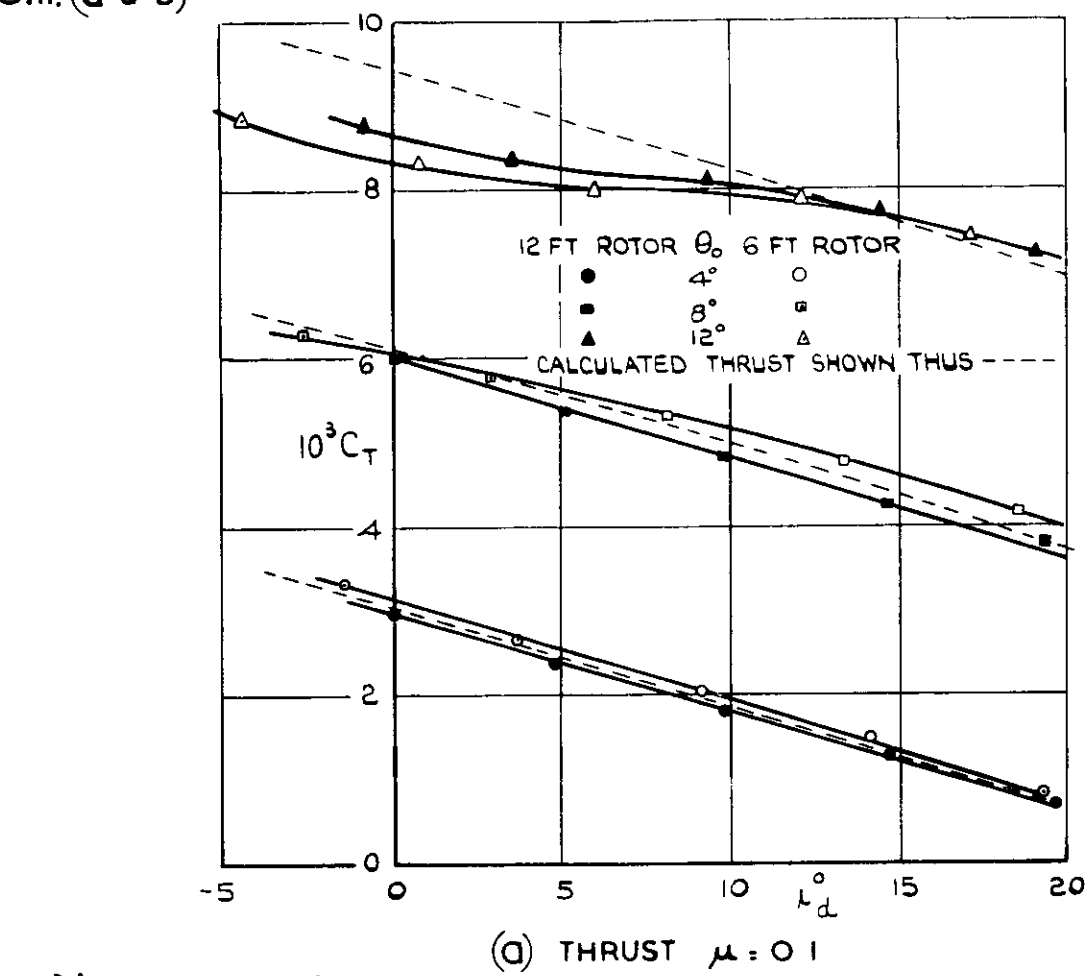

(a) THRUST $\mu = 0.1$

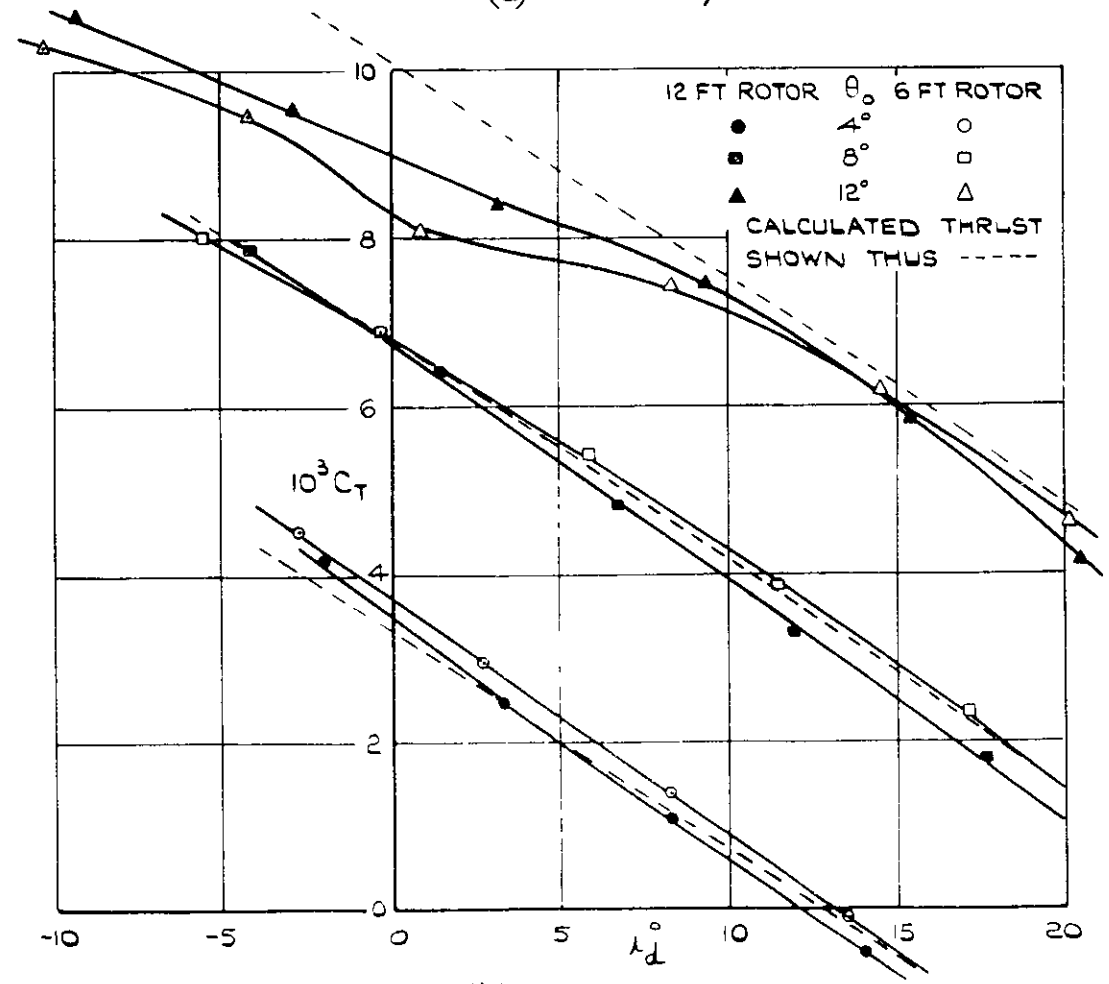

(b) THRUST $\mu = 0.2$

FIG.11. (a & b) COMPARISON OF 12 FT DIA. AND 6 FT DIA. ROTOR THRUST MEASURED IN 24 FT TUNNEL.

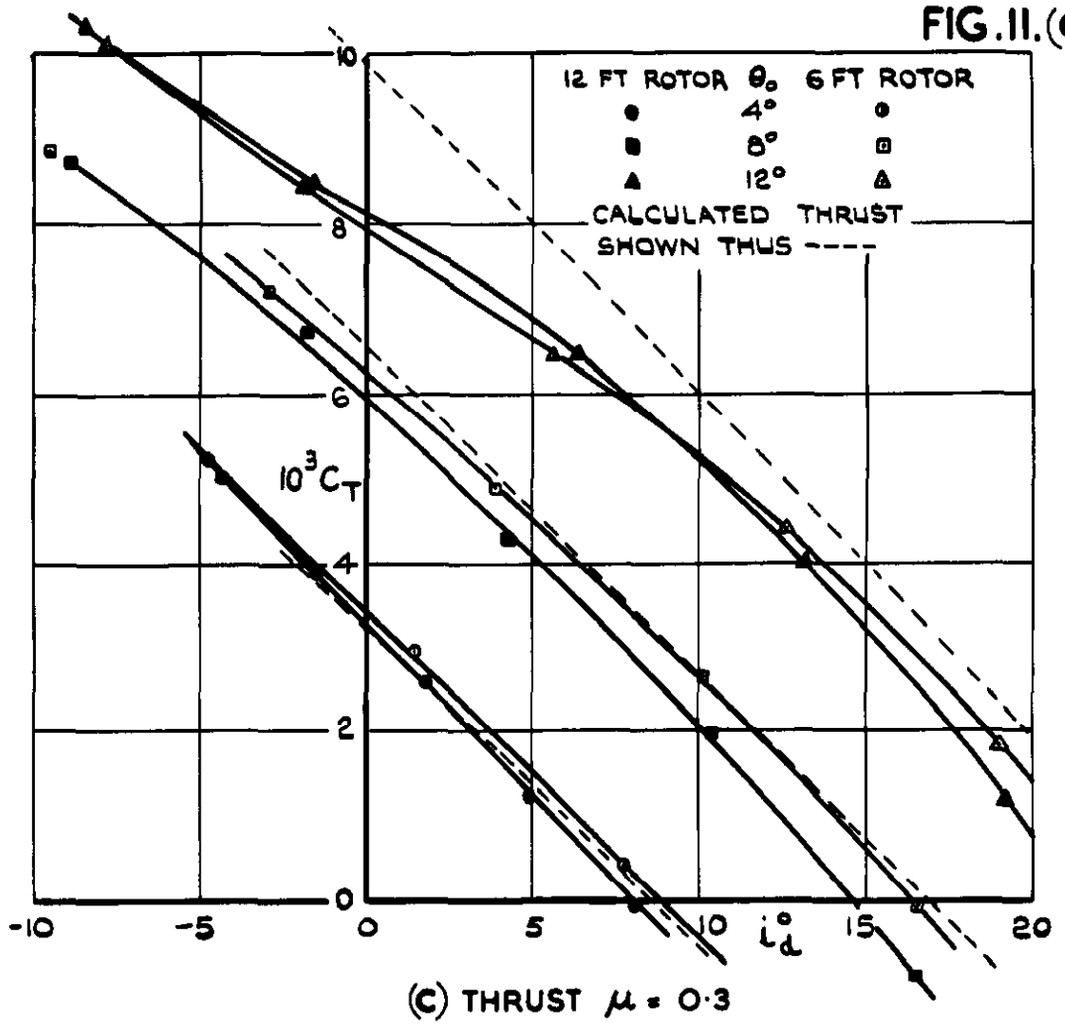

(c) THRUST $\mu = 0.3$

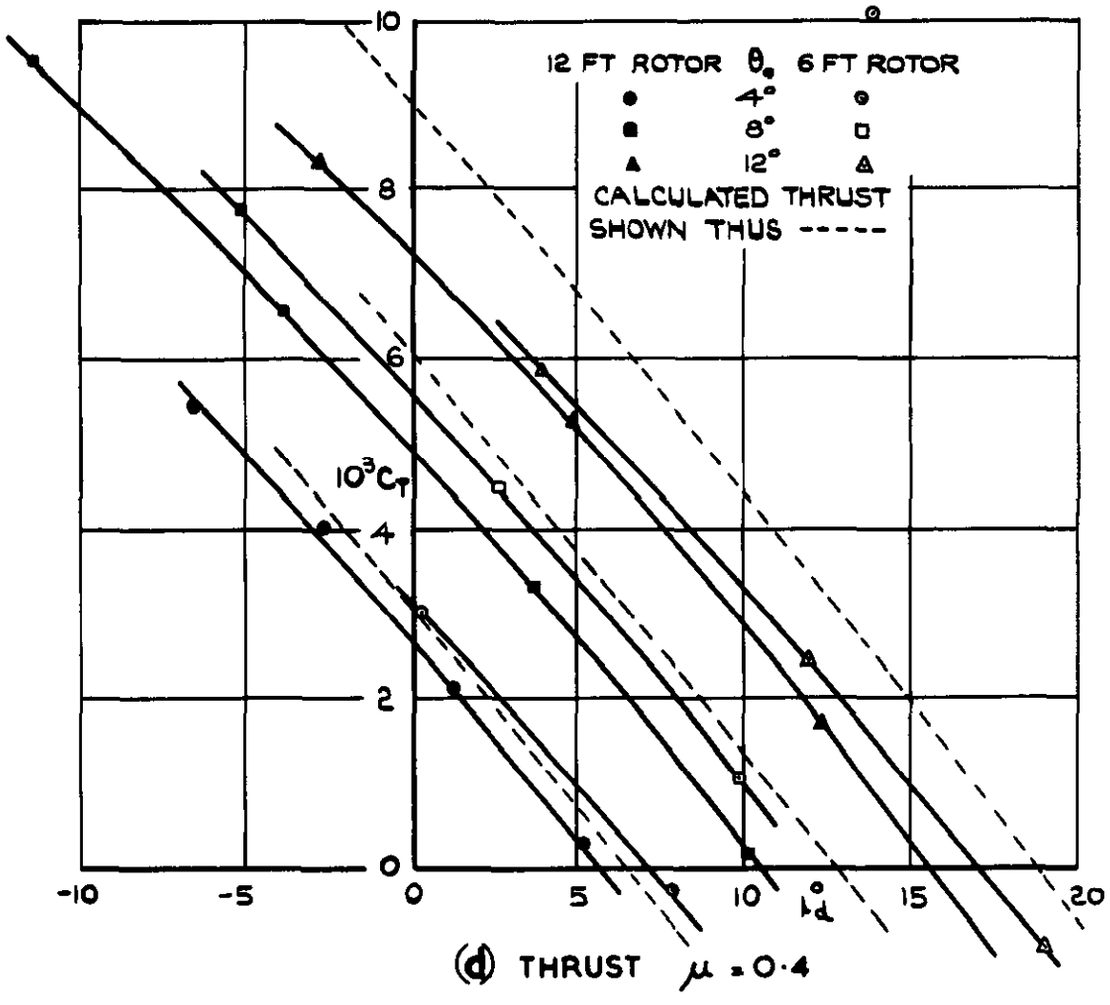

(d) THRUST $\mu = 0.4$

FIG.11. (c & d) COMPARISON OF 12 FT DIA. AND 6 FT DIA. ROTOR THRUST MEASURED IN 24 FT TUNNEL.

FIG. 12. (a & b)

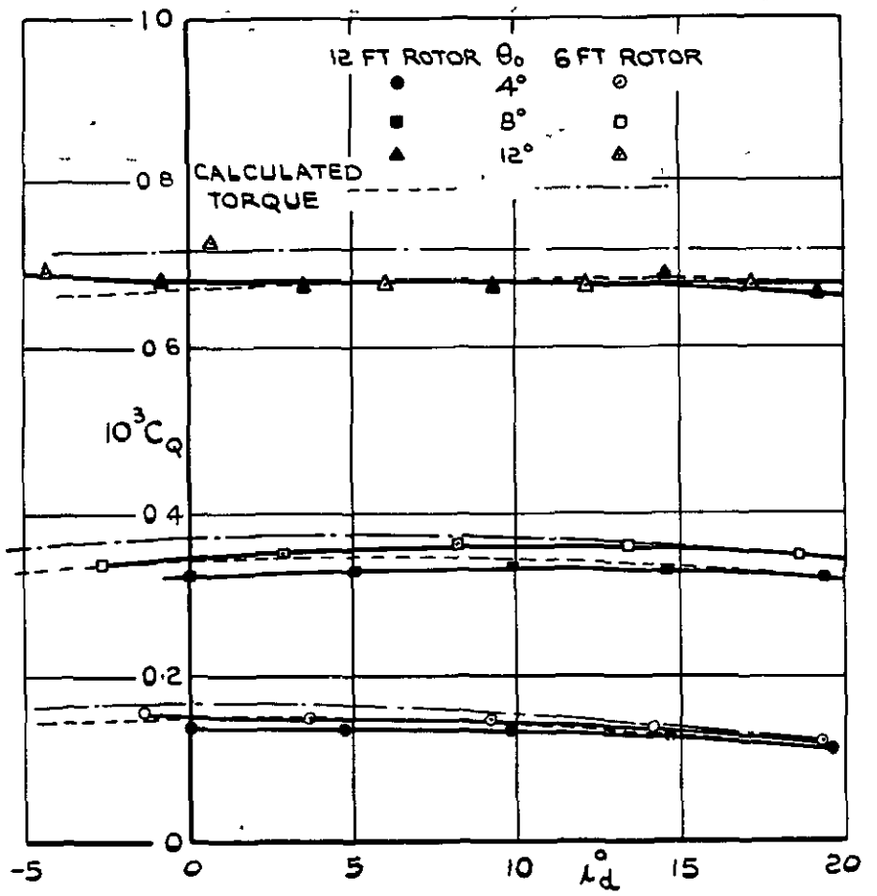

(a) TORQUE $\mu = 0{\cdot}1$

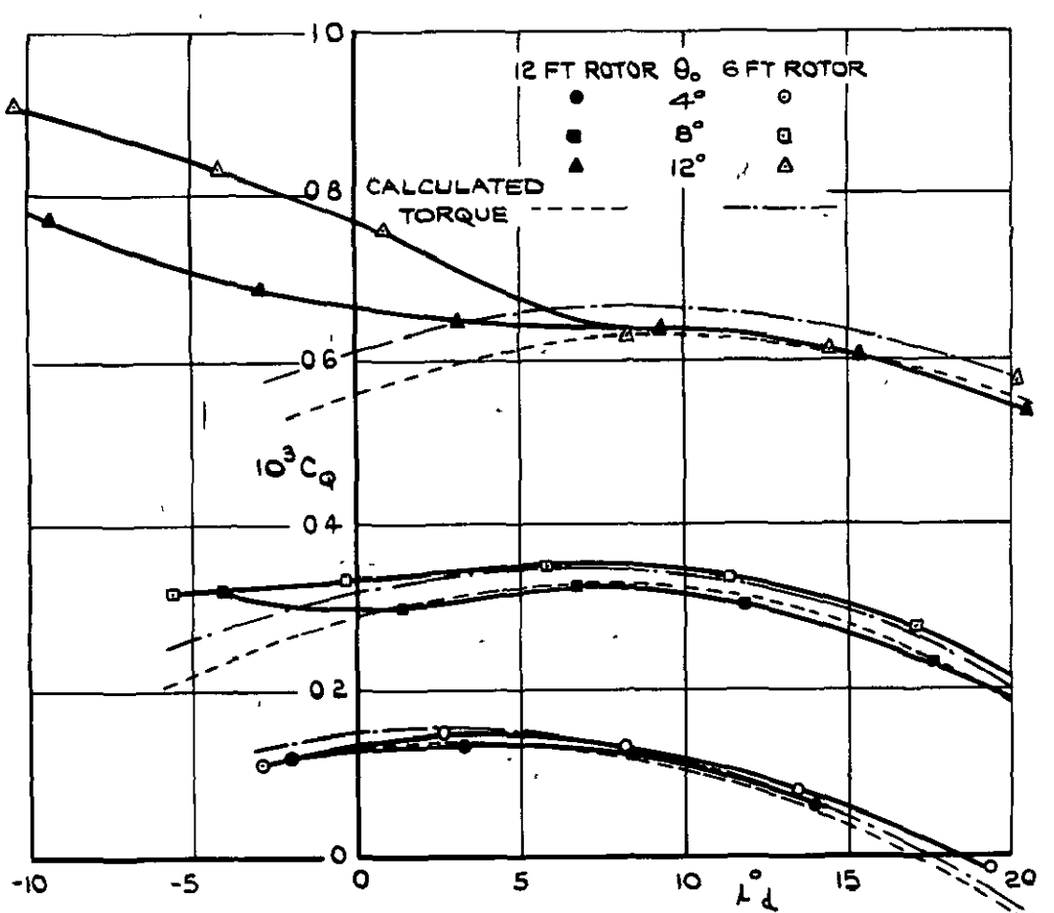

(b) TORQUE $\mu = 0{\cdot}2$

FIG. 12. (a & b) COMPARISON OF 12 FT DIA. AND 6 FT DIA. ROTOR TORQUE MEASURED IN 24 FT TUNNEL.

FIG. 12.(c & d)

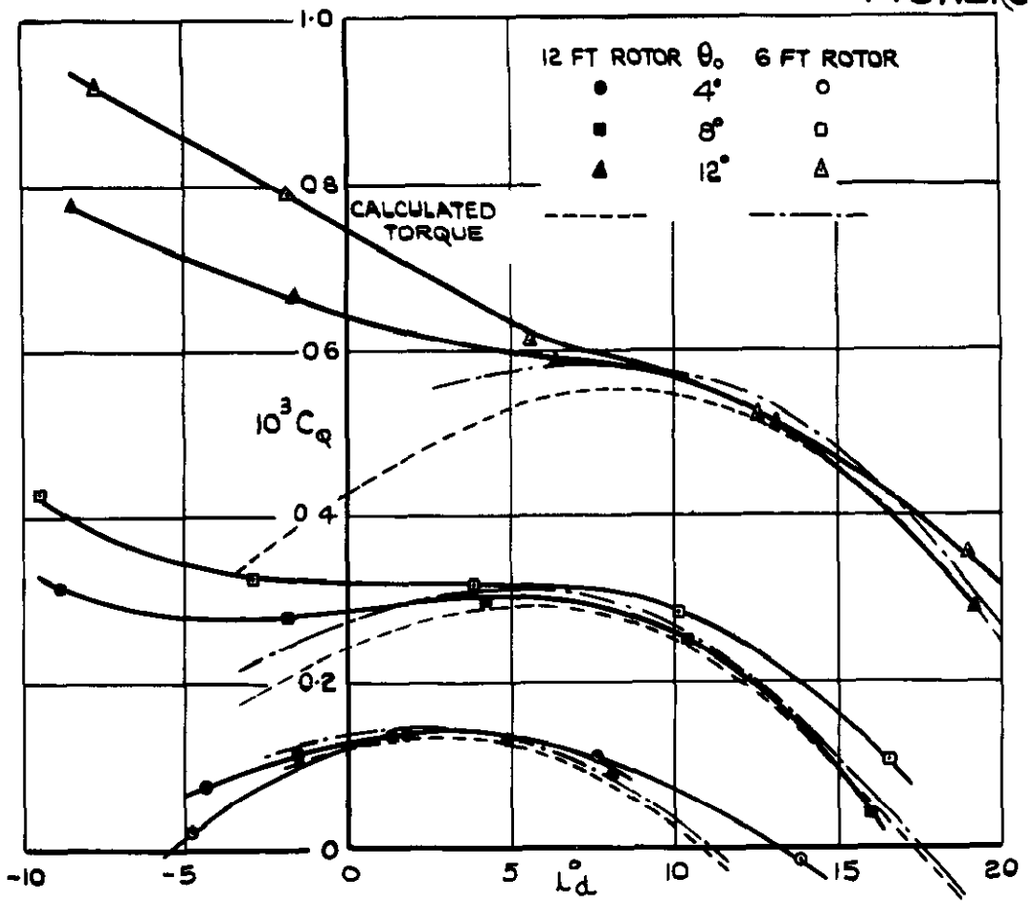

(c) TORQUE $\mu = 0.3$

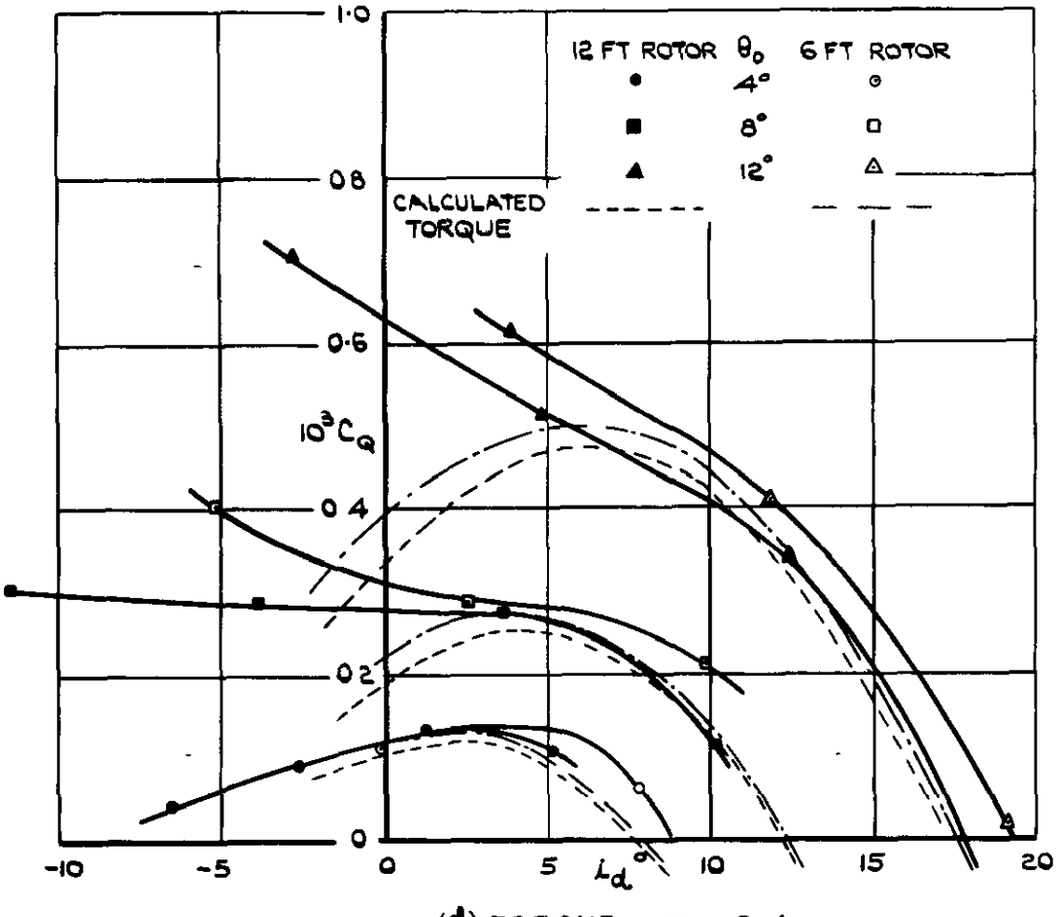

(d) TORQUE $\mu = 0.4$

FIG. 12 (c & d) COMPARISON OF 12 FT DIA. AND 6 FT DIA. ROTOR TORQUE MEASURED IN 24 FT TUNNEL.

FIG.13.(a & b)

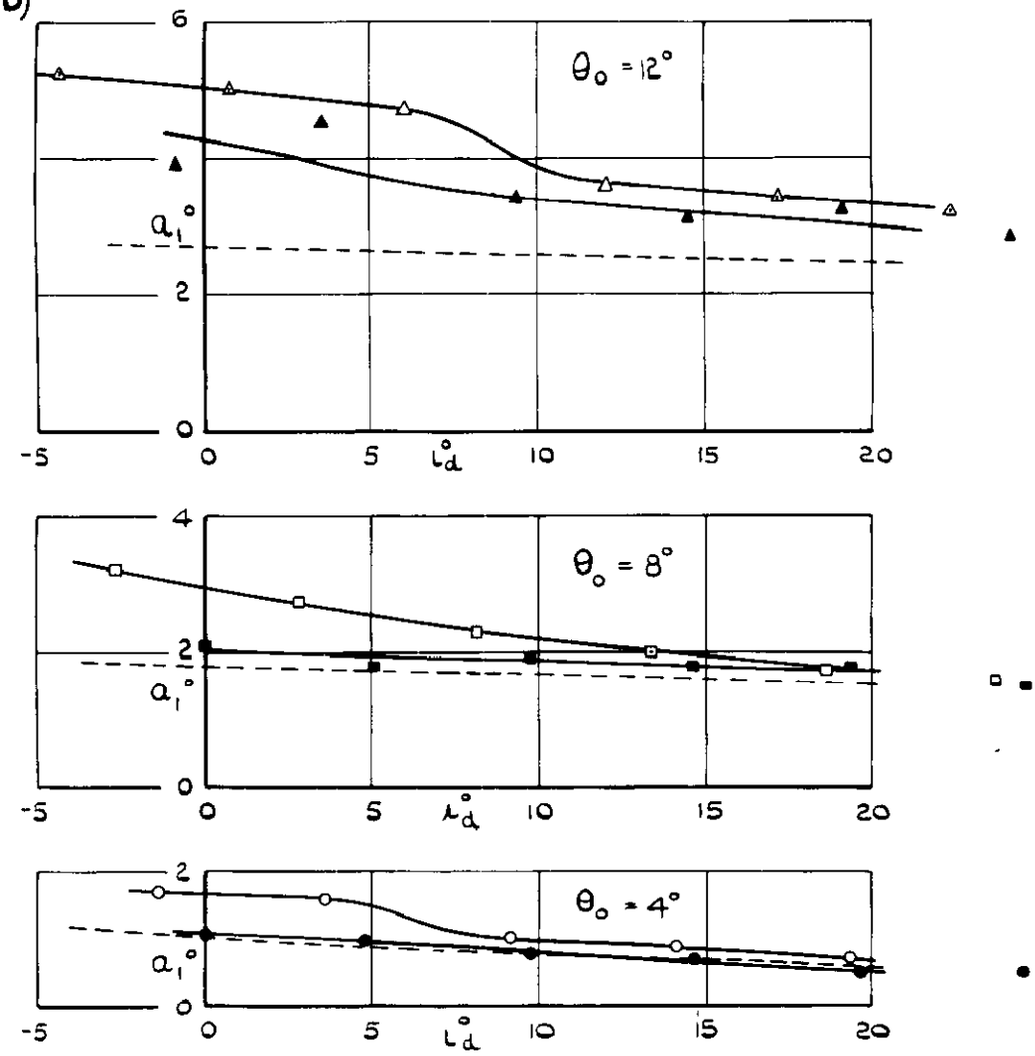

(a) FLAPPING ANGLE $\mu = 0.1$

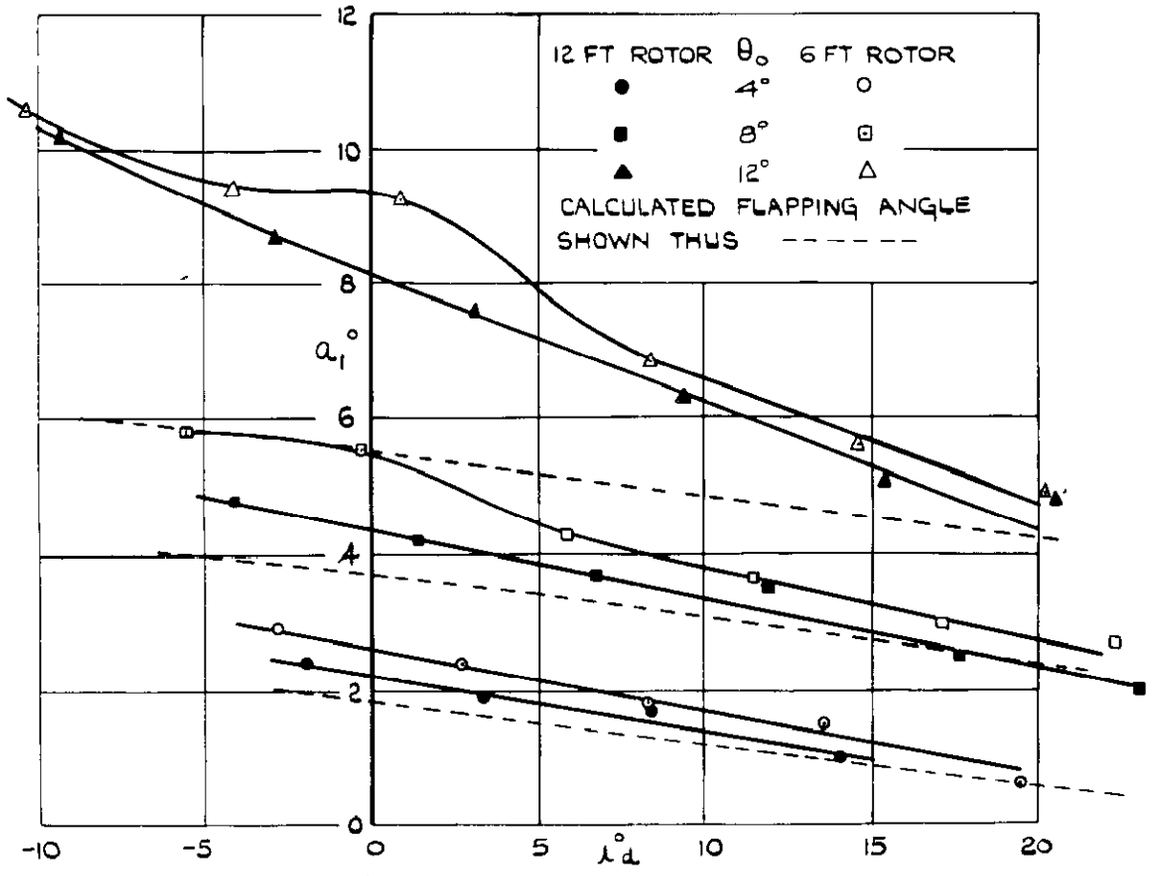

(b) FLAPPING ANGLE $\mu = 0.2$

FIG.13.(a & b) COMPARISON OF 12 FT DIA. AND 6 FT DIA. ROTOR FLAPPING ANGLE MEASURED IN 24 FT TUNNEL.

FIG.13.(c & d)

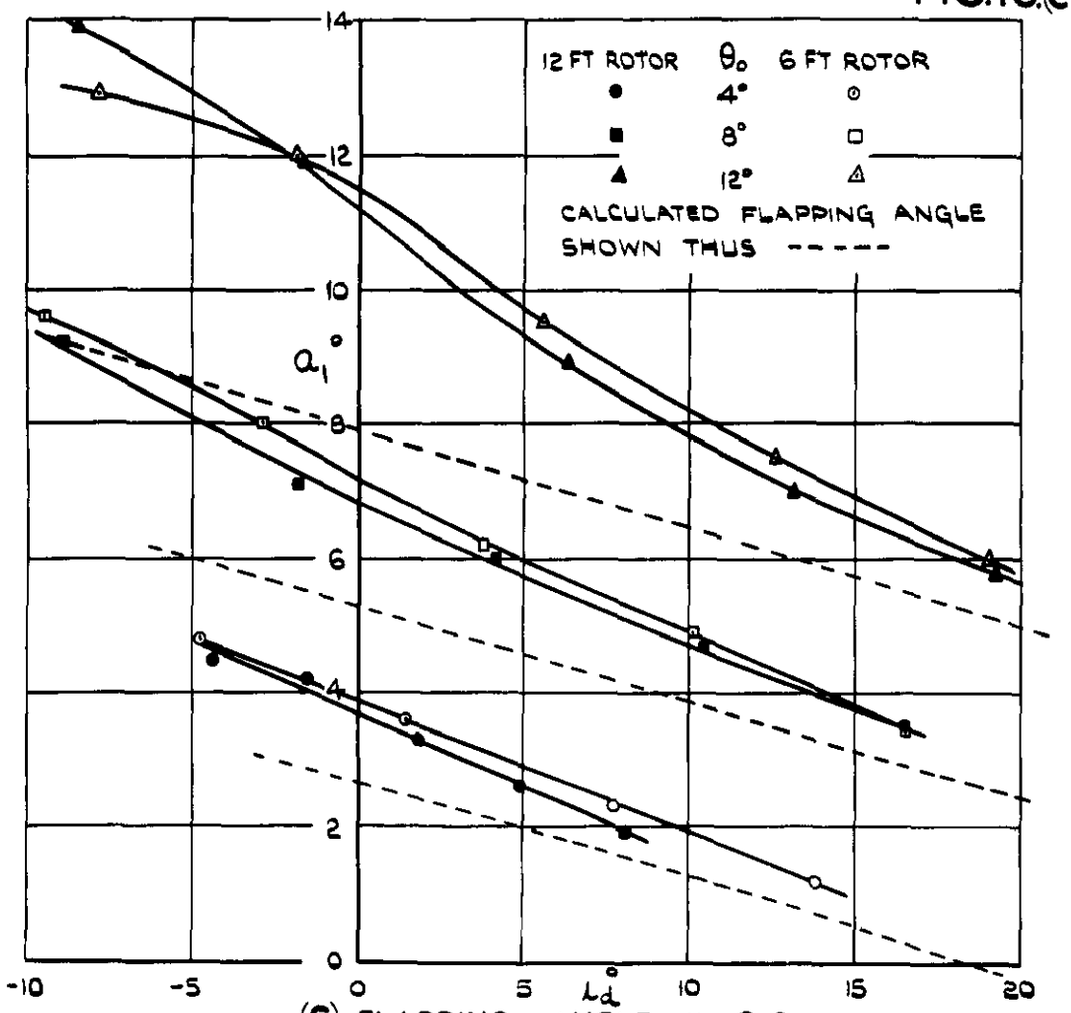

(C) FLAPPING ANGLE $\mu = 0.3$

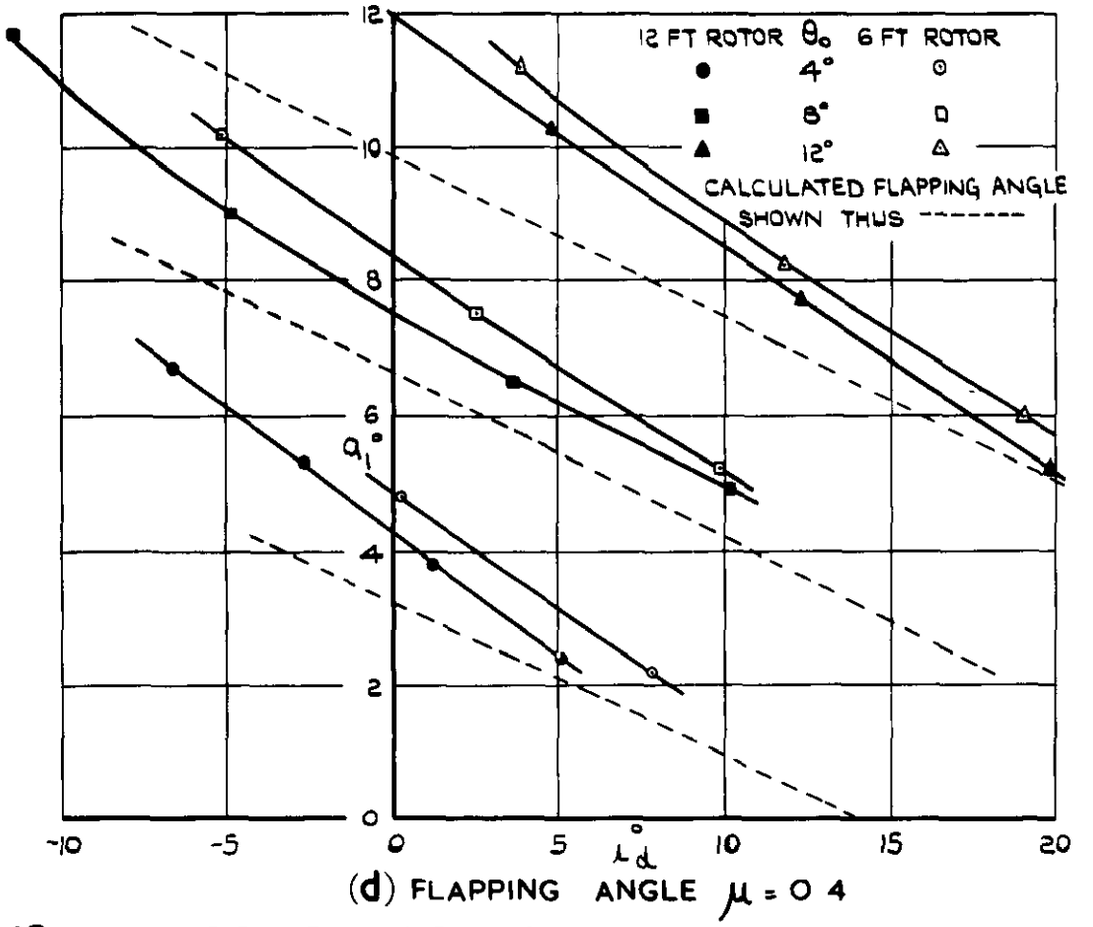

(d) FLAPPING ANGLE $\mu = 0.4$

FIG..13. (c & d) COMPARISON OF 12 FT DIA. AND 6 FT DIA. ROTOR FLAPPING ANGLE MEASURED IN 24 FT TUNNEL.

FIG. 14.(a - c)

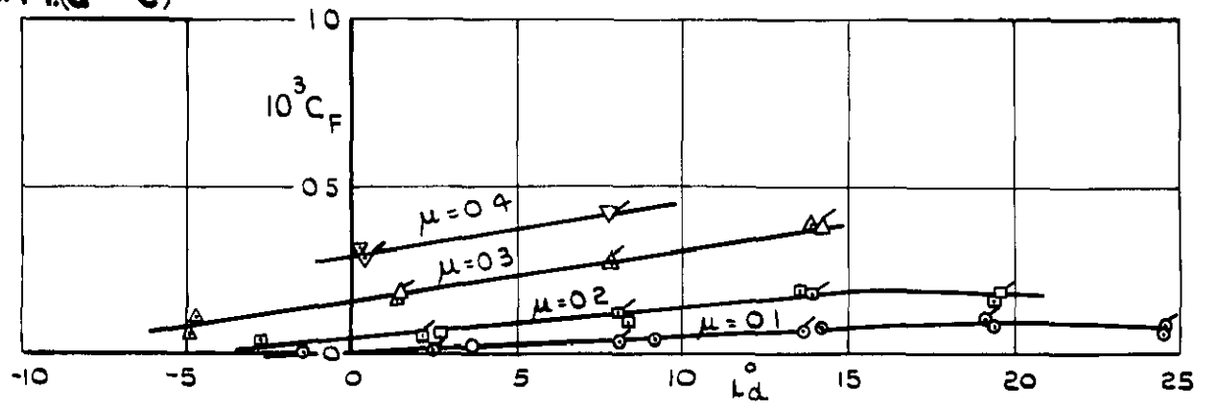

(a) BLADE ANGLE $\theta_0 = 4^\circ$

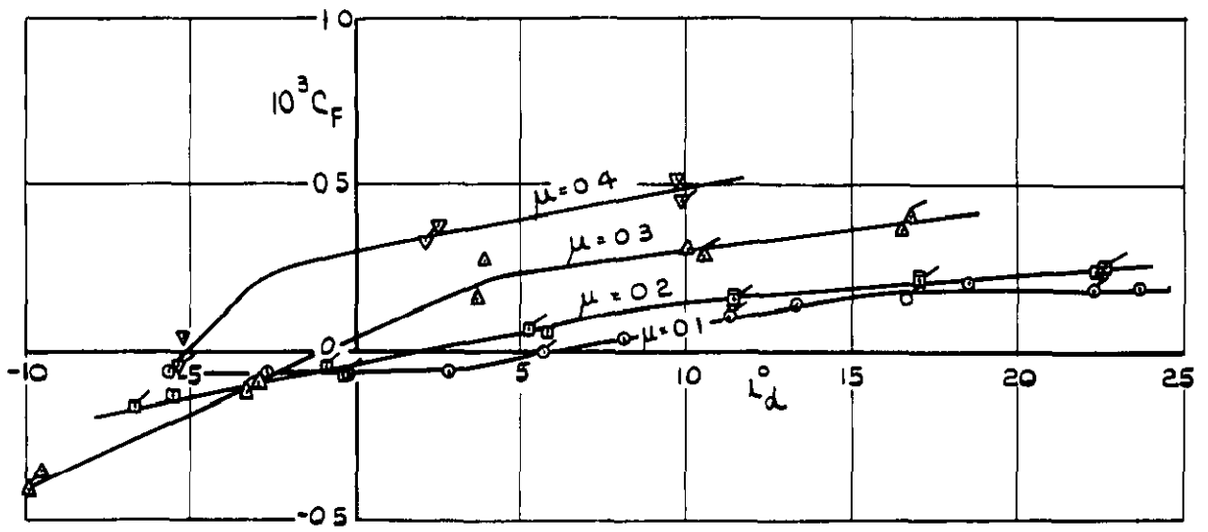

(b) BLADE ANGLE $\theta_0 = 8^\circ$

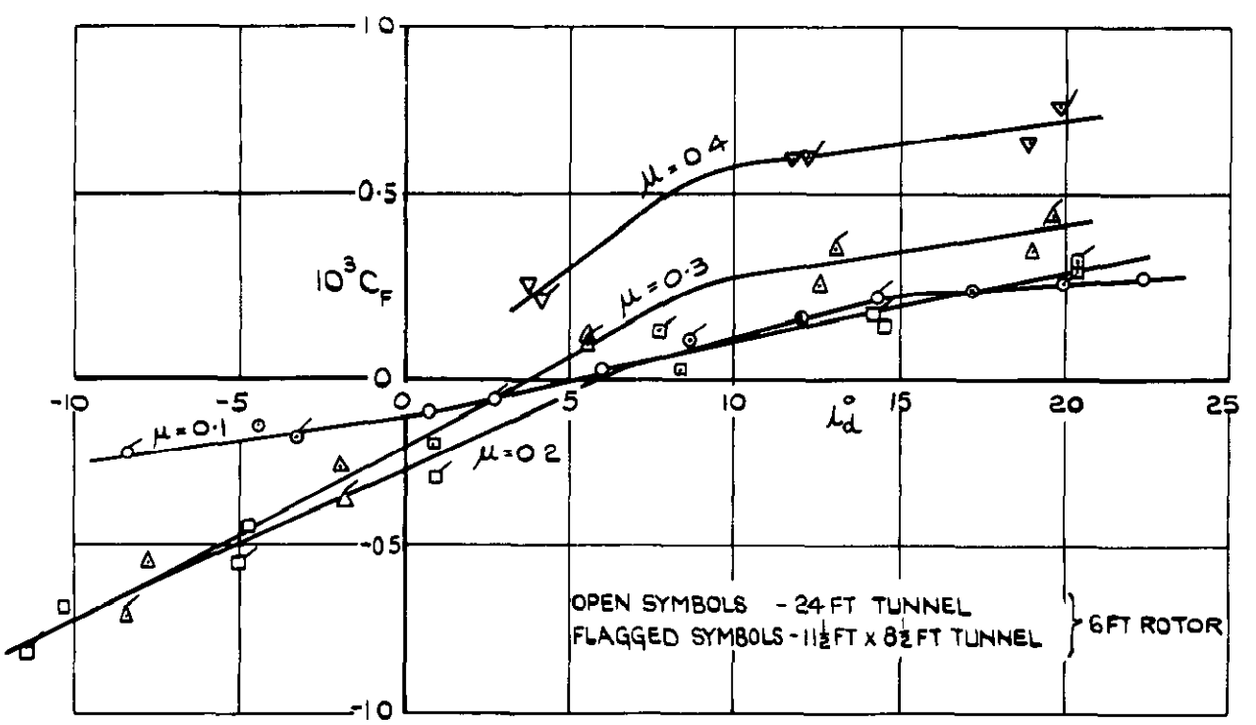

(c) BLADE ANGLE $\theta_0 = 12^\circ$

FIG 14 (a-c) FORCE IN PLANE OF ROTOR DISK. 6 FT DIA. ROTOR IN 24 FT TUNNEL AND $11\frac{1}{2}$ FT X $8\frac{1}{2}$ FT TUNNEL.

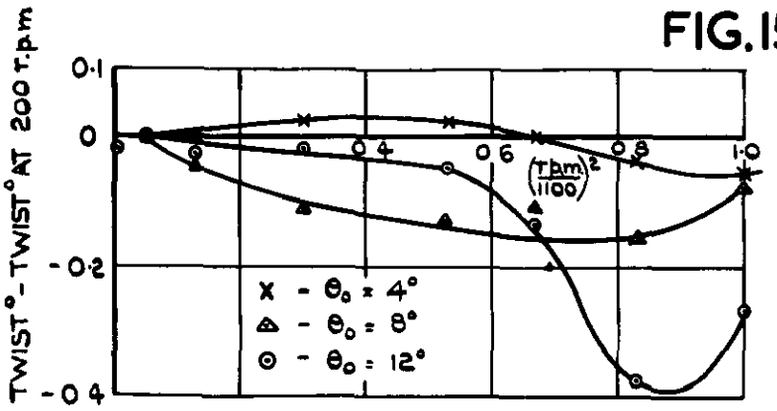

FIG. 15. BLADE TWIST, 6 FT DIA. ROTOR STATIC CONDITION. ($\mu = 0$)

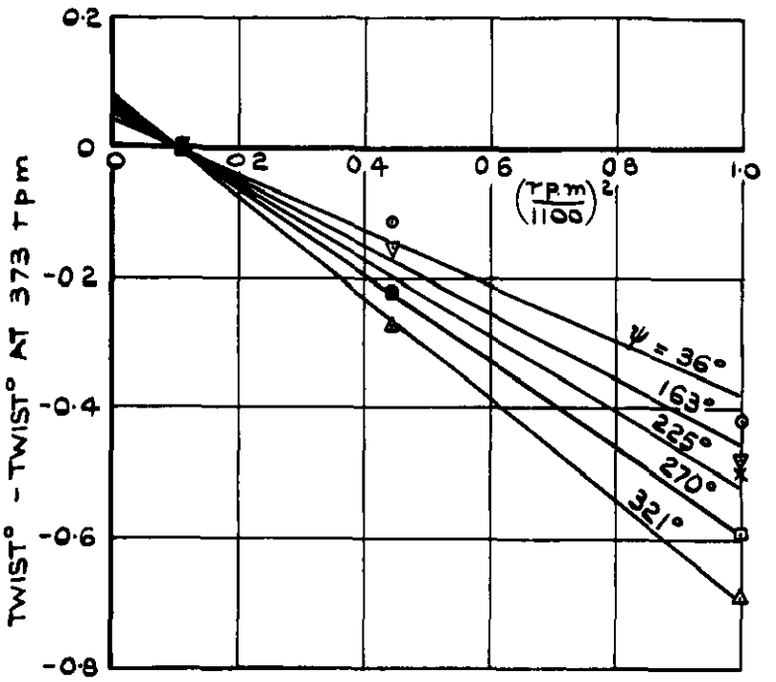

(a) EFFECT OF ROTATIONAL SPEED ON BLADE TWIST.

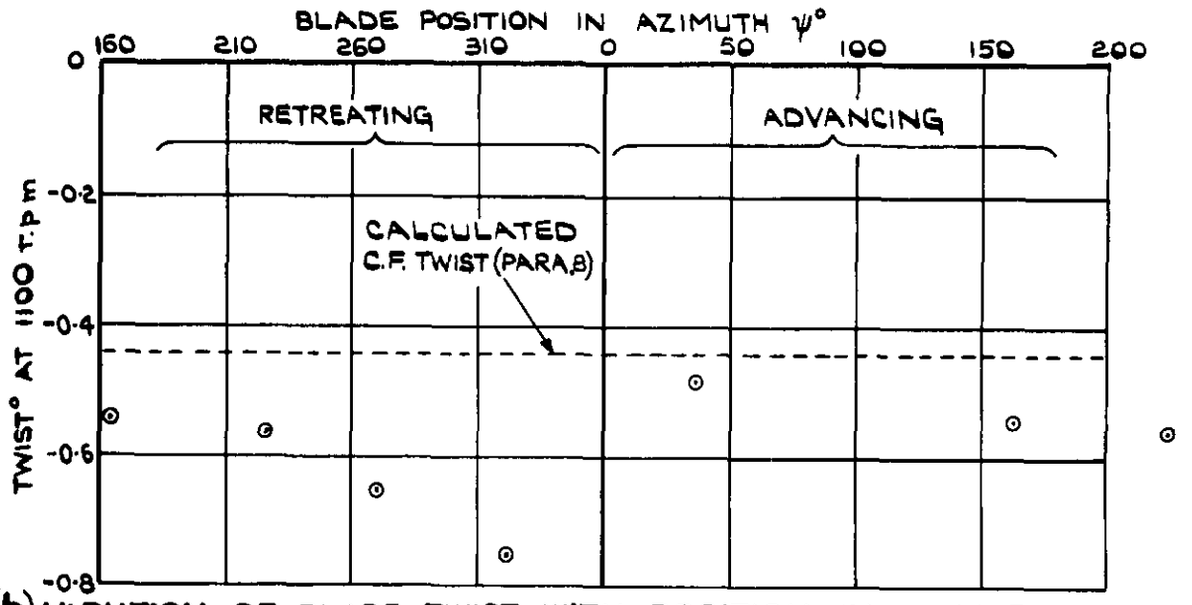

(b) VARIATION OF BLADE TWIST WITH POSITION IN AZIMUTH.

FIG. 16 (a & b) BLADE TWIST 6 FT DIA. ROTOR. (APPROX. ZERO THRUST) $\theta_0 = 8°$, $i_s = 20°$, $\mu = 0{\cdot}3$.

C.P. No. 216
(17,791)
A.R.C. Technical Report

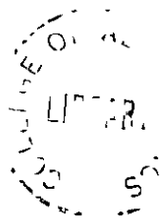

PUBLISHED BY HER MAJESTY'S STATIONERY OFFICE

To be purchased from

York House, Kingsway, LONDON, W.C.2 — 423 Oxford Street, LONDON, W.1
P.O. Box 569, LONDON, S.E.1
13a Castle Street, EDINBURGH, 2 — 109 St. Mary Street, CARDIFF
39 King Street, MANCHESTER, 2 — Tower Lane, BRISTOL, 1
2 Edmund Street, BIRMINGHAM, 3 — 80 Chichester Street, BELFAST
or from any Bookseller

1955

Price 3s. 6d. net

PRINTED IN GREAT BRITAIN

S.O. Code No. 23-9009-16

C.P. No. 216